



## UNIVERSITY OF NAIROBI

### FACULTY OF ENGINEERING

### DEPARTMENT OF ELECTRICAL AND INFORMATION ENGINEERING

**DESIGN AND OPTIMIZATION OF A WIRELESS POWER TRANSFER SYSTEM  
FOR LOW-POWER DEVICES USING RESONANT INDUCTIVE COUPLING**

**PROJECT INDEX: PRJ 131**

**SUBMITTED BY: ANDITI IMELDA JUTTA**

**REGISTRATION NUMBER: F17/1744/2019**

**SUPERVISOR(S): PROF. HEYWOOD OUMA**

**MR. KINYUA WACHIRA**

**EXAMINER: DR. GEVIRA OMONDI**

This project is submitted in partial fulfilment of the requirement for the award of the Degree of Bachelor of Science in Electrical and Electronic Engineering at the University of Nairobi

**SUBMITTED ON: 4<sup>TH</sup> JUNE 2025**

## **DECLARATION**

This Research Proposal is my original work and has not been presented before any panel in any university for the degree of Bachelor of Science in Electrical and Electronic Engineering.

ANDITI IMELDA JUTTA

F17/1744/2019



04/06/2025

Signature

Date

This project has been submitted for examination with my approval as University Supervisor.

PROF. HEYWOOD OUMA

.....  
Signature

.....  
Date

MR. KINYUA WACHIRA

.....  
Signature

.....  
Date

## **ACKNOWLEDGEMENT**

First and foremost, I give all glory and thanks to God Almighty for His grace, provision and strength throughout the course of this project. Without Him, none of this would have been possible.

I am grateful to my supervisors, Mr. Kinyua Wachira and Prof. Heywood Ouma, for their consistent support, expert guidance, and valuable feedback throughout the development of this work which has been instrumental in shaping both the technical direction and academic quality of this project.

My heartfelt appreciation goes to my parents, Mr. and Mrs. Anditi, for their unwavering support and encouragement. Your belief in me has been my greatest motivation. To my dearest friend, Mark and sisters, Grace, Liv, and Claudia; thank you for being my constant pillars, my greatest friends, and the support system I have leaned on through every phase of this journey. Your presence has given me the strength to push forward.

I also wish to thank my classmates for the teamwork and shared learning experiences that have enriched both my academic and personal growth.

This project is a reflection of all the encouragement, support, and love I have received from those around me, and I am truly thankful.

## ABSTRACT

This project report presents the design, implementation, and experimental evaluation of a wireless power transfer (WPT) system for low-power applications using resonant inductive coupling. The objective was to eliminate the need for physical connectors in power delivery, offering a more convenient and flexible energy transfer solution for small electronic loads.

The system has been divided into two primary subsystems: a transmitter, powered by a 12 V DC supply and controlled by an Arduino UNO generating complementary PWM signals to drive an H-bridge inverter; and a receiver, consisting of a resonant coil, a parallel compensation capacitor, a full-bridge rectifier, and a smoothing capacitor connected to a low-power load. Both the transmitter and receiver coils were manually wound and tuned to resonate at approximately 100 kHz, using compensation capacitors to form resonant LC tanks.

Key experiments focused on the impact of coil alignment, air-gap distance, and orientation on the output voltage and transfer efficiency. Results showed that under optimal conditions—coils aligned face-to-face at about 40 mm separation—the system consistently delivered around 5V DC to the load, achieving a power transfer efficiency of up to 40%. Misalignment and increased separation led to notable performance degradation, confirming the sensitivity of resonant coupling to geometric factors.

The findings validate resonant inductive coupling as an effective technique for short-range wireless power delivery in low-power applications. Recommendations for future work include closed-loop control, automatic frequency tuning, and integration of wireless communication for smarter, more adaptive WPT systems.

## TABLE OF CONTENTS

ACKNOWLEDGEMENT .....	iii
ABSTRACT.....	iv
TABLE OF CONTENTS.....	v
LIST OF TABLES.....	viii
LIST OF FIGURES .....	ix
LIST OF ABBREVIATIONS.....	x
Chapter 1: INTRODUCTION.....	1
1.1 Background.....	1
1.2 Problem Statement.....	1
1.3 Project Justification.....	2
1.4 Objective .....	3
1.4.1 Specific Objectives .....	3
1.5 Scope of the Project .....	3
Chapter 2: LITERATURE REVIEW.....	5
2.1 Wireless Power Transfer.....	5
2.2 Far Field Wireless Power Transfer .....	5
2.2.1 Microwave Power Transfer.....	5
2.2.2 Laser Power Transfer .....	6
2.3 Near Field Power Transfer.....	7
2.3.1 Inductive Power Transfer.....	7
2.3.2 Capacitive Power Transfer.....	10
2.4 Fundamentals of Inductively Coupled Wireless Power Transfer Systems.....	10
2.4.1 Operating Principle of Inductively Coupled Wireless Power Transfer Systems (ICWPTs).....	11

2.4.2 ICWPT System Tuning.....	13
2.5 Resonant Inductive Coupling.....	16
2.5.1 Resonant Inductive Coupling Topologies.....	16
2.6 Coil Design Optimization for Maximum Efficiency .....	21
2.6.1 Optimizing Coil Structure for Maximum Efficiency.....	21
2.6.2 Selecting Optimal Coil Materials to Maximize Efficiency.....	24
2.6.3 Proposed Coil Design Optimization Methods for Maximum Efficiency .....	26
Chapter 3: DESIGN AND IMPLEMENTATION.....	28
3.1 System Overview .....	28
3.2 Design Goals and Requirements .....	30
3.3 Theory of Resonant Inductive Coupling.....	31
3.3.1 Resonant Frequency.....	31
3.3.2 Quality Factor and Link Efficiency .....	32
3.4 Transmitter Sub-System.....	33
3.4.1 Power Supply Rails.....	34
3.4.2 PWM Generation (Arduino UNO).....	35
3.4.3 Gate Driver Stage (IR2110) .....	36
3.4.4 H-Bridge Inverter.....	38
3.4.5 Series-Compensated Transmitter Tank.....	39
3.5 Receiver Sub-System .....	41
3.5.1 Parallel-Compensated LC .....	41
3.5.2 Rectifier and Filter .....	42
3.5.3 Load Interface .....	43
3.6 Component Selection Justification .....	43
Chapter 4: RESULTS AND ANALYSIS .....	46

4.1 Circuit Realization and Test Setup .....	46
4.2 Effect of Coil Orientation on Power Transfer.....	47
4.3 Effect of Air-Gap Distance on Power Transfer .....	49
4.4 Prototype Development .....	50
4.4.1 Transmitter Prototype Design .....	50
4.4.2 Receiver Prototype Design .....	51
Chapter 5: CONCLUSION AND RECOMMENDATIONS.....	52
5.1 Conclusion .....	52
5.2 Recommendations.....	52
5.3 Final Remarks .....	54
APPENDICES .....	55
REFERENCES .....	60

## **LIST OF TABLES**

Table 2. 1 Comparison between the Helix and Spiral Coil Structures .....	22
Table 3. 1 Main Design Requirements and Sub-System Responsibility .....	30
Table 3. 2 Power Rails Specifications .....	34
Table 3. 3 Key IR2110 Specifications and Rationale for Use .....	38
Table 3. 4 Electrical Characteristics of IRFZ44N .....	39
Table 3. 5 Main Component Choices with Justification.....	45
Table 4. 1 Receiver Output Voltage at Different Coil Orientations .....	47
Table 4. 2 Effect of Coil Separation on Received Output Voltage.....	49

## **LIST OF FIGURES**

Figure 2. 1 Classification of Wireless Power Transfer Systems.....	5
Figure 2. 2 Functional Blocks of a General Inductive Power Transfer System .....	8
Figure 2. 3 Fundamental Theory of an Inductively Coupled WPT System.....	11
Figure 2. 4 Typical Flux Linkage in Inductively Coupled WPT Systems.....	12
Figure 2. 5 Elements of an ICWPT System .....	13
Figure 2. 6 primary Side Tuning Topologies.....	14
Figure 2. 7 Series-Series Topology.....	17
Figure 2. 8 Series-Parallel Topology .....	18
Figure 2. 9 Parallel-Parallel Topology .....	19
Figure 2. 10 Parallel-Series Topology .....	19
Figure 2. 11 LCL-LCL Compensation Topology .....	20
Figure 3. 1 Simplified Model of the WPT System .....	28
Figure 3. 2 System-level Flowchart .....	29
Figure 3. 3 Graph of Efficiency vs. k plotted for various Q .....	33
Figure 3. 4 Transmitter Sub-System Schematic .....	33
Figure 3. 5 Arduino code showing Timer1 configuration for 100kHz complementary PWM generation.....	36
Figure 3. 6 Receiver Sub-System Schematic .....	41
Figure 4. 1 Experimental Setup of the WPT System.....	46
Figure 4. 2 Coils placed at 45 degrees .....	48
Figure 4. 3 Experimental Setup for d=10mm .....	49
Figure 4. 4 Experimental Setup for d=70mm .....	50
Figure 4. 5 Receiver Section.....	51

## **LIST OF ABBREVIATIONS**

<b>Abbreviation</b>	<b>Full Term</b>
AC	Alternating Current
DC	Direct Current
ICWPT	Inductively Coupled Wireless Power Transfer
RIC	Resonant Inductive Coupling
Rx	Receiver
Tx	Transmitter
WPT	Wireless Power Transfer

# **Chapter 1: INTRODUCTION**

## **1.1 Background**

Nikola Tesla is regarded the pioneer of Wireless Power Transfer, in 1891, he designed the Tesla coil, a device about forty meters long powered by a 300kW signal at a frequency of 150kHz and could transmit electricity up to three kilometers without using wires [1], [2]. Subsequent experiments in the field of WPT were carried out by various other scientists and researchers in the following years, in 1894 for example, Hulin and LeBlanc proposed an apparatus for powering an electric vehicle inductively using an AC generator[2], in Japan 1962, Yagi and Uda developed a system which transferred power wirelessly through coupling antennas acting as resonators[1]. In 2007, a research group at the Massachusetts Institute of Technology designed a resonant inductive coupled WPT system which enabled transmission of electricity enough to ignite a 60W bulb at a distance of two meters [1], [2]. Some of the first commercial products integrated with WPT systems are electric toothbrushes, shavers and inductive wireless chargers for wireless telephones. Over the years, WPT techniques have gained researchers' and industry attention as a result of the increasing number of battery-powered devices such as computers, electric vehicles, mobile phones, sensors, mainly as a way to replace the standard cable charging but also as a way of powering battery-less equipment [3].

WPT operational principles are divided into two, that is electromagnetic coupling WPT (near-field WPT) that uses high frequency magnetic or electric fields and uncoupled WPT (radiative WPT) that transfers power via radio waves.

## **1.2 Problem Statement**

Wireless Power Transfer has emerged as a transformative technology with the potential to revolutionize how electronic devices are powered [4]. By eliminating the need for physical connectors, WPT offers significant advantages, including increased convenience, reduced wear and tear on ports, and enhanced usability in environments where wired connections are hazardous or impossible [3]. Major drawbacks of WPT systems include low power transfer efficiencies, sensitivity to coil alignment, high cost and limited transfer distance [4], [5]. In this project, these drawbacks are countered by using resonant inductive coupling that offers better efficiency even over longer transfer distances compared to standard inductive coupling technique [4]. Coil design

is also optimized through solutions focusing on Tx and Rx coil structures, shapes and materials in order to achieve maximum transfer efficiency and offer tolerance to misalignment and variations in distances between the transmitter and receiver coils [4]. High power transfer efficiency has the overall effect of making the system more economical [3]. Regarding WPT, each application requires several self-specific transfer characteristics. The most important transfer characteristics are power transfer efficiency, value of the output power, mutual position between the transmitter and receiver, and their geometric dimensions [3]. Influencing these parameters lies in the main circuit configuration of a compensation network and the optimal design of the coils of the system. In comparison with standard inductively coupled systems, resonant inductively coupled systems offer several other significant advantages which this project explores, these are their low environmental impact and their ability to be tuned based on the requirements of target applications [3].

### 1.3 Project Justification

The global shift towards device miniaturization, automation, and user convenience is driving a growing demand for wireless power transfer systems. This project focuses on the design of a WPT system using resonant inductive coupling to efficiently power low-power devices. The optimization of coil design plays a central role in achieving high power transfer efficiency while addressing practical challenges associated with WPT systems. The benefits of the proposed system include:

- i. Increased Efficiency – The transmitter and receiver coils have been designed to operate at optimal resonant frequencies ensuring stable and efficient power transfer. High quality Litz wire is used to fabricate the coils reducing coil conduction losses ensuring better efficiency. The coil structures have been carefully selected, choosing coil geometries that maximize the coupling coefficient between the coils and thereby improving transfer efficiency.
- ii. Extended Range of Power Transfer – Resonance enables power transfer over greater distances allowing for greater flexibility in device placement.
- iii. Low Maintenance Requirement – By eliminating physical connectors, the system's maintenance needs are reduced and the lifespan of devices is extended. WPT allows for sealing of devices thereby reducing the risk of corrosion by water or chemical agents.

- iv. Compactness – Optimized coil designs reduce the size and weight of the WPT system. The system allows for the design of much smaller and lighter devices by opting out bulky batteries.
- v. Enhanced User Convenience – By eliminating cables and connectors, the system simplifies device operation and enhances user experience. The inconvenience of having many wires sharing a limited number of power sockets is solved. Spaces are made tidier and more organized by eliminating the clutter caused by physical connectors around power outlets.
- vi. Improved Safety – The absence of exposed wires reduces risks of electrical shocks
- vii. Sustainability – Efficient energy transfer achieved through resonant coupling and coil design optimization minimizes energy waste contributing to eco-friendly design principles.

The project's outcomes have the potential to revolutionize device usability, improve energy efficiency and drive innovation in wireless power transfer technology, aligning with modern demands for convenience, sustainability and functionality.

## 1.4 Objective

To design a wireless power transfer system using resonant inductive coupling

### 1.4.1 Specific Objectives

- i. To make a transmitter and a receiver coil
- ii. To demonstrate the system powering a low-power device
- iii. To demonstrate automatic power cutoff in the case of coil misalignment

## 1.5 Scope of the Project

The system will be optimized for a single receiver device, this is because supporting multiple devices would involve complex tuning and advanced algorithms which are not feasible within the project timeline.

The project will be limited to short-range power transfer as extending the range would require advanced coil designs that are beyond the project's budget and regulatory compliance that requires higher expertise.

Compliance with WPT standards for consumer-grade systems may not be fully addressed as these require specialized testing facilities. Electromagnetic interference management might not be addressed due to time constraints and the level of expertise required.

# Chapter 2: LITERATURE REVIEW

## 2.1 Wireless Power Transfer

Wireless power transfer is the transfer electrical power from one point to another through an air gap without any direct electrical contacts [3]. A typical WPT system consists of a transmitter (Tx) and a receiver (Rx). WPT is used integrated in applications such as electric vehicles (EVs), consumer electronics, biomedical equipment etc. where conventional wires are inconvenient, hazardous, unwanted, or impossible [3]. WPT is divided into two categories dependent on the mechanism of energy transmission [2].

- i. Near Field Power Transfer also known as the non-radiative method
- ii. Far field wireless power transfer

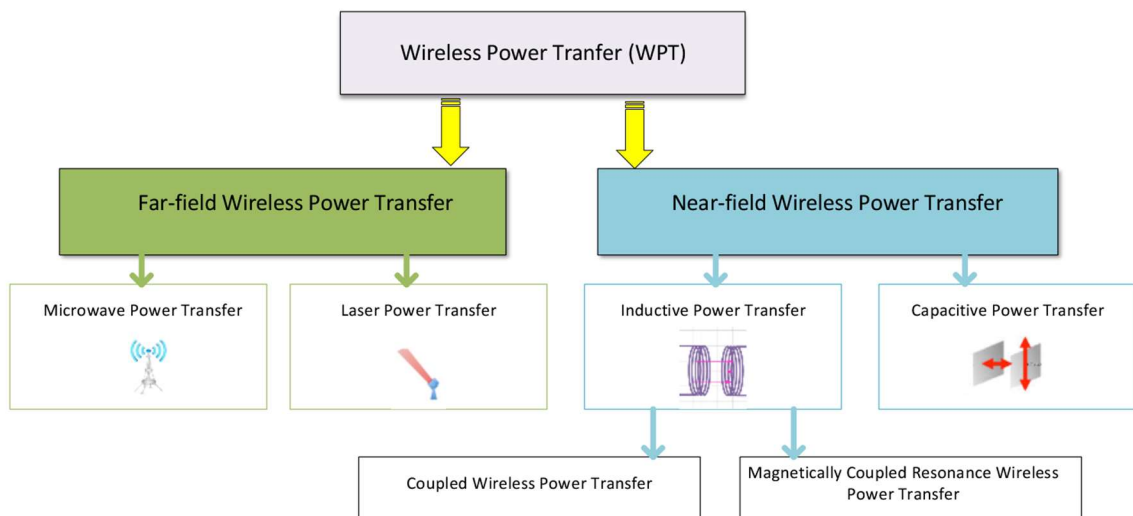


Figure 2. 1 Classification of Wireless Power Transfer Systems

## 2.2 Far Field Wireless Power Transfer

Uses an electromagnetic wave in the form of a radio frequency signal for energy transfer. The transmitter then radiates energy using the electric field of the electromagnetic wave [2].

### 2.2.1 Microwave Power Transfer

Wireless transmission of energy is carried out by electromagnetic radiation with the use of microwaves. Based on the use of microwave devices for radiating signals in the form of radio

waves through antennas. In the receiver(antenna), the energy stored in the electric field of the wave is transferred to the load.

### **Applications**

Mostly used where there is a need to supply devices located at long distances apart and operating in different weather conditions [2] for example:

- i. Aviation industry to supply unmanned ships

### **Advantages**

- i. Has the potential to transfer several kW
- ii. Good adaptation to the environment
- iii. Great flexibility in transmitting and receiving signals
- iv. Long effective transmission distance of up to several km

### **Limitations**

- i. Low transmission efficiency not exceeding 10% [2]
- ii. Very expensive
- iii. Requires large antennas

#### **2.2.2 Laser Power Transfer**

The transmitter (Tx) converts electrical energy from a source such as a battery to a monochromatic light beam using a laser. This beam is then directed at the energy receiver (Rx) which is usually a set of photovoltaic panels placed on satellites to obtain the highest possible transmission efficiency over very long distances. In the receiver which is adapted to the parameters of the beam, energy of the laser radiation is converted back to electrical energy used to charge batteries on the satellites or power motors installed in the location.

### **Advantages**

- i. Long effective transmission distance of up to several km
- ii. Potential to transfer several kW

### **Limitations**

- i. Complex tracking and monitoring systems required to precisely transmit the laser beam to the receiver
- ii. Laser radiation poses health risks to humans and can have a negative impact on the environment
- iii. Susceptible to atmospheric absorption and scattering by clouds, rain etc.
- iv. Low transmission efficiency of less than 20%

### 2.3 Near Field Power Transfer

Involves power transfer via a magnetic or electric field and is the most developed Wireless Power Transfer technology [2]. Near field power transfer is classified into two categories [2], that is:

- i. Inductive Power Transfer (IPT)
- ii. Capacitive Power Transfer (CPT)

A general IPT system is characterized by a transmitter and a receiver coil and a generalized CPT system consists of two capacitors, one acting as the transmitter and the other as a receiver.

Near Field Power Transfer has found applications in:

- i. Implantable medical devices
- ii. Charging of portable electronics such as smart phones
- iii. Underwater robots and sensors
- iv. Electric Vehicles (EVs)

#### 2.3.1 Inductive Power Transfer

The principle of power transmission is based on the operation of a transformer. An AC voltage source is connected to the terminals of the primary winding, in this case the transmitter. Time varying magnetic flux is created as a result inducing emf in the secondary winding (receiver) and causing current flow. This transformer action is described by Ampere's and Faraday's Laws of electromagnetic induction.

#### Main Components of a General IPT System

The functional blocks of a general inductive power transfer system are illustrated in Figure 2.2

- i. Rectifier – converts AC voltage from an external power source into a DC voltage of the required value depending on application
- ii. DC/AC Inverter – converts DC voltage to AC voltage
- iii. Transmitter Coil
- iv. Receiver Coil
- v. Regulator – stabilizes the voltage at the receiver output
- vi. Compensation block – consists of capacitors connected in various configurations to the transmitter and receiver to create a resonant circuit

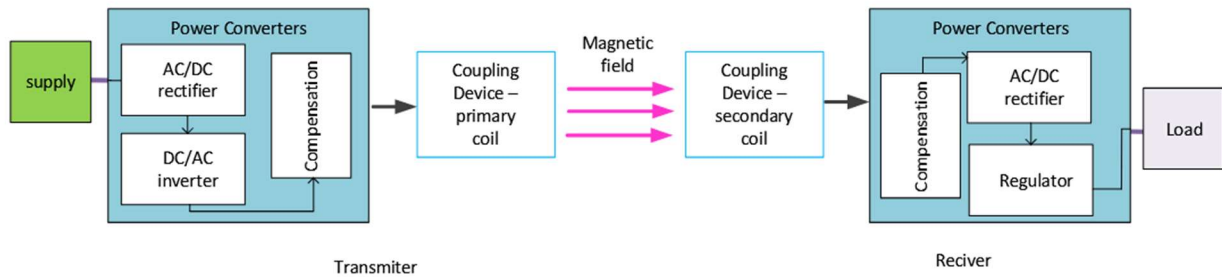


Figure 2. 2 Functional Blocks of a General Inductive Power Transfer System

## Advantages

- i. It is possible to obtain high transmission efficiency (up to 90%)
- ii. Capability to transfer high power (up to several kW)
- iii. Good galvanic isolation
- iv. Can be used in a range of applications, from powering small devices such as smart phones to large devices such as electric vehicles

## Limitations

- i. Power can be transferred over a limited distance (from cm to m)
- ii. Significant eddy current losses limit areas of application

IPT can further be classified into the following two subgroups:

- i. Inductive Coupled Wireless Power Transfer
- ii. Magnetically Coupled Resonance Wireless Power Transfer

## Inductive Coupled Wireless Power Transfer

Power is transferred by means of magnetic field of transmitter and receiver coils coupled together at a short distance from each other. The operating frequency is in the range of kHz and typical distance between the transmitter and receiver does not exceed 40mm, power transferred is in the range of single watts to kW [2].

Increasing distance between Tx and Rx from 20mm to 100mm reduces the coupling coefficient, k from 0.6 to 0.1 and the power transfer efficiency from 80% to 40% [2]. The value of k and transmission efficiency is influenced by such factors as the number of turns of the coils, the shape and the size of the coils.

### **Advantages**

- i. It is a simple method of power transfer
- ii. High transmission efficiency
- iii. Low operating frequency ensuring safety of energy transmission

### **Limitations**

- i. Power can only be transferred over a short distance
- ii. Heating of systems as a result of losses in the coils
- iii. Power transmission efficiency variations depending on position of coils in relation to each other

### **Magnetically Coupled Resonance Wireless Power Transfer**

The principle of power transformer is similar to the action of an air transformer. The resonant frequency at which both coils operate is very key and the frequency of operation ranges from a few kHz to tens of MHz. Power transfer can be achieved over distance of several metres regardless of weather conditions [2]. The position between Tx in relation to the position of Rx influences the coupling factor k between the coils therefore affecting efficiency of power transmission. The quality factor, Q, which characterizes losses from the coils is dependent on the coil sizes, thickness of the wire forming the coils and material of the wire [2]. High Q results in better properties of the WPT system.

### 2.3.2 Capacitive Power Transfer

Capacitive power transfer uses the capacitive coupling between the Tx and Rx which are electrodes of a capacitor in the form of metal plates. The transmitter system is powered by an AC voltage which in turn causes the appearance of an AC potential transmitted to the load on receiver plates.

#### **Advantage**

- i. Costs less since metal plates are used as transmitter and receiver
- ii. High power transfer capability (up to several kW)
- iii. Power is transferred without the generation of eddy currents

#### **Limitations**

- i. Power transfer is limited to very short distances between transmitter and receiver plates (max 100mm)
- ii. CPT is a less secure technology
- iii. Limited transmission efficiency in the range of 70-80%

#### **Applications**

- i. Used to power small-sized devices such as medical implants
- ii. Used to power reconfigurable systems or robot arms due to its flexibility and small size

## 2.4 Fundamentals of Inductively Coupled Wireless Power Transfer Systems

ICWPTs provide power to moveable objects across a gapped magnetic structure [3]. Designing a magnetic coupling structure with small air gap would result in high magnetic coupling coefficient and increase power transfer capability. The magnetic structure of ICWPTs combine magnetic properties of both an ideal transformer and an inductor. In order to reduce skin and proximity effects associated with coils, multi-strand-woven Litz wire is used. In the design, analysis and modelling of switch-mode non-linear circuits are a main concern [3]. Typical Inductively Coupled Wireless Power Transfer Systems are made up of [3]:

- i. Loosely coupled magnetic coupling structure
- ii. Power electronics circuitries as an integrated system

#### 2.4.1 Operating Principle of Inductively Coupled Wireless Power Transfer Systems (ICWPTs)

Inductively Coupled Wireless Power Transfer systems' operation is based on Faraday and Ampere's Laws [3]. Figure 2.3 illustrates the fundamental operation of ICWPTs based on these laws. A current  $I$  flowing through a conductor generates a magnetic field  $H$  around it. The magnetic field links the secondary power pickup coil and according to Faraday's Law causes a voltage  $V$  to be induced. Ampere's law states that the line integral of the magnetic field intensity around a closed loop is equal to the current flowing through it and is expressed mathematically as:

$$\oint \vec{H} \cdot d\vec{l} = I \quad (1)$$

Faraday's Law is expressed mathematically as:

$$V = -N_2 \frac{d\phi}{dt} \quad (2)$$

Where  $N_2$  is the number of turns of the secondary coil

The negative sign in (2) is described by Lenz's Law which states that current flow in the secondary coil (when a load is connected) will be such that it creates a magnetic field that opposes the primary magnetic field.

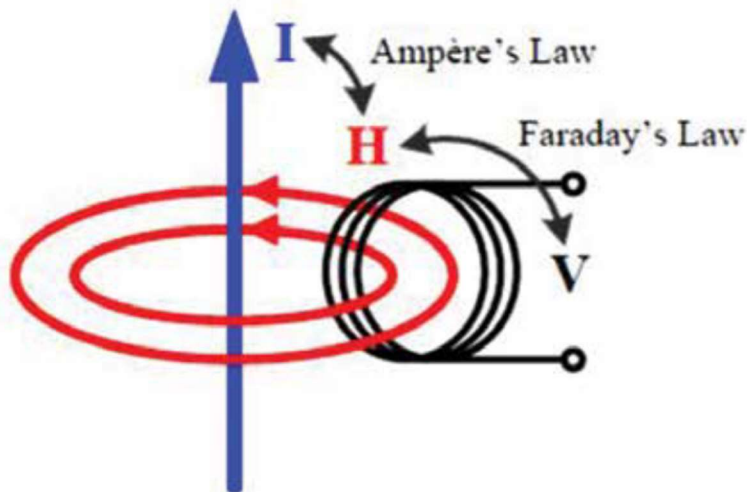


Figure 2.3 Fundamental Theory of an Inductively Coupled WPT System

In an ICWPT system, direct physical contacts are eliminated and a magnetic link is used to provide reliable and efficient power transfer across an air gap [3].  $\Phi_m$ , which is the mutual flux, couples from one half of the core to the other half and provides mutual inductance,  $M$  that couples energy

from the primary to the secondary side as illustrated in Figure 2.4.  $M$  is a function of geometry [3] and can be determined by simulation, measurement or modelling the physical structure.

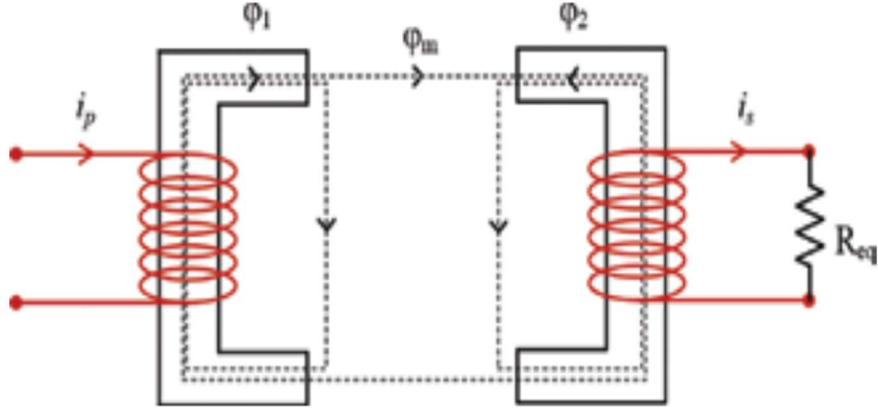


Figure 2.4 Typical Flux Linkage in Inductively Coupled WPT Systems

In such a loosely coupled power transfer system, the leakage fluxes can be very large and cannot be ignored [3]. The proportion of primary coil's flux that links with the secondary coil is known as the primary coupling coefficient denoted as  $k_1$  and given by the expression:

$$k_1 = \frac{\phi_M}{\phi_1} \quad (3)$$

The secondary coupling coefficient  $k_2$  is given by:

$$k_2 = \frac{\phi_M}{\phi_2} \quad (4)$$

The primary and secondary coupling coefficients combined give the overall system  $k$  expressed as:

$$k = \sqrt{k_1 k_2} \quad (5)$$

The mutual inductance,  $M$  between the primary and secondary coils is given by:

$$M = k \sqrt{L_p L_s} \quad (6)$$

Where  $L_p$  and  $L_s$  are self-inductances of the primary and secondary coils respectively

Figure 2.5 is an illustration of the basic elements of an ICWPT system:

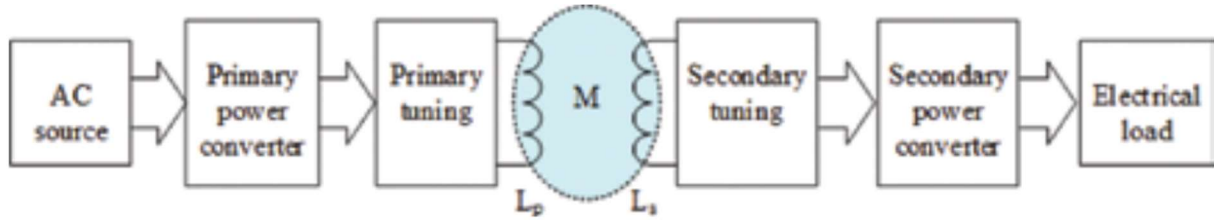


Figure 2. 5 Elements of an ICWPT System

The primary side AC/DC/AC resonant converter converts rectified AC power into high frequency AC power. The secondary side of the system can be moveable (linearly or/and rotating) giving flexibility, mobility and safety for supplied loads [3]. The secondary converter converts and controls induced high frequency power to meet the requirements specified by the load parameters. Time varying magnetic field generated by the primary coil induces an emf in the secondary coil which forms the voltage source of the secondary power supply. The magnetic coupling of an ICWPT system is very loose compared to that of normal transformers [3] so that the induced voltage source is unsuitable to be used to drive the load directly. Power conditioning with proper circuit tuning and conversion is therefore required to control the output power according to load requirements [3].

#### 2.4.2 ICWPT System Tuning

Tuning the primary and secondary inductances of an ICWPT system is important because of the following reasons [3]:

- i. Compensating the primary inductance makes the power supply able to drive given limited voltage ratings of employed switches
- ii. Constructing a resonant tank for resonant converters required to enable soft-switching operation of the switches hence reducing switching losses and Electromagnetic Interference (EMI)
- iii. Prevents harmonic propagation in the circuit due to its filtering action
- iv. Compensating the secondary inductance improving the power transfer capability of the system

#### Primary Side Tuning

Compensating the primary inductance improves the power factor and reduces the required Volt-Ampere rating of the primary power source [3]. Compensation topologies for achieving primary side tuning are as illustrated in Figure 2.6 :

- i. Series Compensation
- ii. Parallel compensation
- iii. Series-Parallel Compensation

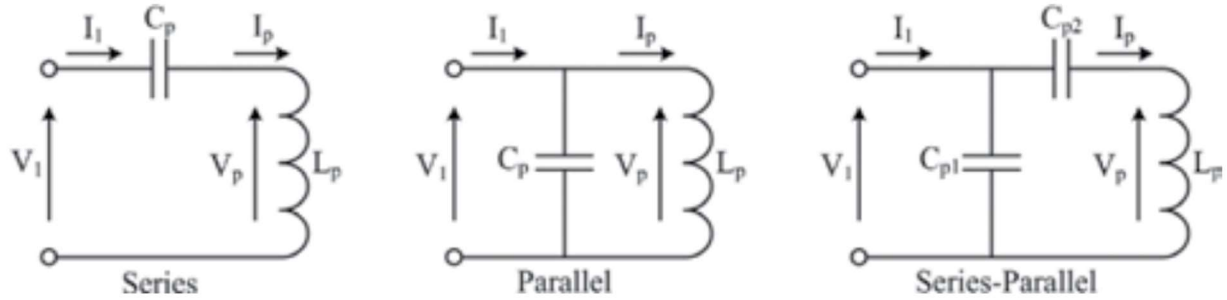


Figure 2.6 primary Side Tuning Topologies

### i. Series Compensation

The output current from the inverter bridge ( $I_1$ ) is equal to the primary current  $I$  passing through the primary inductance ( $L_p$ ). This signifies that the primary current in series compensation circulates through the inverter bridge which in turn causes significant power dissipation in the switching network. The voltage in series compensation is boosted because of the added voltage across the tuning capacitance. This results in an increased voltage across the primary coil ( $V_p$ ) that is higher than the inverter output voltage ( $V_1$ ). This is beneficial as it allows the power supply to drive a high primary inductance with a desired primary current [3].

### ii. Parallel Compensation

Parallel compensation has a current increase property [3].  $I_p$  is greater than the power converter output current ( $I_1$ ), this is because the reactive current is circulating inside the resonant tank and only the real current is flowing through the inverter bridge. As a result, in a parallel tuned power supply design, lower current rated switches may be used. The value of the primary compensation capacitance is designed to fully compensate the primary inductance at the primary operating angular frequency ( $\omega$ ). In this case, the primary compensation capacitance is given by:

$$C_p = \frac{1}{\omega^2 L_p} \quad (7)$$

Equation (7) gives the primary compensation capacitance for either a series or a parallel tuning topology.

### iii. Series-Parallel Compensation

In this composite topology,  $C_{p2}$  fully cancels the primary leakage reactance ( $L_p - M$ ) and  $C_{p1}$  fully tunes the remaining portion of the primary self-inductance.

$$C_{p1} = \frac{1}{\omega^2 M} \quad (8)$$

$$C_{p2} = \frac{1}{\omega^2 (L_p - M)} \quad (9)$$

## Secondary Side Tuning

In an ICWPT system because of large internal reactance, power transferred from the primary to the secondary side is not sufficient for the load [3]. In the case of an uncompensated secondary inductance, maximum output power is achieved when the load resistance,  $R_L$  is equal to the internal reactance,  $\omega L_s$ , [3] that is:

$$P_{o,max} = \frac{1}{2} V_{oc} I_{sc} \quad (10)$$

where  $V_{oc}$  is the open-circuit voltage at the secondary terminals and  $I_{sc}$  is the short circuit current of the secondary side.

To improve the power transfer capability of the system, the secondary side is tuned to primary side operating frequency [3]. Two basic tuning topologies used in the secondary side are:

- i. Series Compensation
- ii. Parallel Compensation

In the circuit diagrams below,  $R_{eq}$  denotes the equivalent load on the secondary side

### i. Series Tuning

In series tuning, the equivalent reactance and its compensation capacitance cancel each other at the **resonant frequency** making the output voltage independent of the load and equal to the secondary open-circuit voltage.

## ii. Parallel Tuning

The equivalent admittance and its compensating capacitance cancel each other at the resonant frequency making the output current independent of the load and equal to the secondary short circuit current. For **maximum power transfer, the secondary resonant frequency is usually designed to equal the nominal frequency**.

In this case, the secondary compensation capacitance is determined as:

$$C_s = \frac{1}{\omega^2 L_s} \quad (11)$$

## 2.5 Resonant Inductive Coupling

Resonant Inductive Coupling is more efficient than standard inductive coupling due to the use of strong coupling of the resonant Tx and Rx coils that consequently maximizes power transfer efficiency for even greater distances between the coils [6]. Resonant coupling aims to reduce the required voltage and/or current for power transfer [7]. RIC is used in applications such as EV battery charging, Implantable Medical Devices and mobile device charging. RIC is being studied for use in slip-ring applications and battery-less sensor systems [8]. Compensation circuits in the Tx and Rx sections are essential [7] for:

- i. Achieving proper impedance matching
- ii. Compensating leakage inductances
- iii. Achieving resonance between the Tx and Rx coil

### 2.5.1 Resonant Inductive Coupling Topologies

There are four main circuit topologies to achieve resonant inductive coupling in wireless power transfer system, these are the series-series (SS), series-parallel (SP), parallel-parallel (PP) and the parallel-series (PS) topologies [9]. Each topology involves connecting the primary and secondary coils in different connections that are tuned to resonate at the switching frequency to improve the overall efficiency of the system [9], [10]. Power transfer efficiency depends on the frequency of

operation of the WPT system and the mutual inductance between the coils [10]. The selection of primary and secondary compensation capacitances is based on two criteria [9] which are:

- i. Choosing a secondary capacitance to compensate for the secondary leakage inductance and mutual inductance. This aims to improve the power transferred to the load.
- ii. Selecting a primary capacitance while considering the inductance of the entire wireless power transfer system

The primary parallel compensation resonant inductive links, that is the PP and PS topologies often require an additional series inductance to manage the current coming into the primary resonant circuit from the power amplifier [8]. Due to inductor conduction losses, adding another series inductance reduces efficiency in these topologies. The value of the primary compensation capacitance in PP and PS topologies fluctuates with mutual coupling and load necessitating sophisticated control procedures [8]. In the SS and SP topologies an extra inductor is not required and the main compensation is load-independent [8]. WPT systems with SS or PP compensation networks present current source characteristics [11].

### **Series-Series Topology**

Compensating capacitances are inserted in series to the transmitter and receiver coils. The series-series topology allows for a higher coupling coefficient and increased power transfer efficiency [9]. However, the voltage across each coil is additive which may require higher voltage handling capabilities. The SS topology has been in the systems of [8], [10]. [8] argues that in consideration of system efficiency, component count and control complexity, an SS resonant inductive link is theoretically the best for battery-less applications.

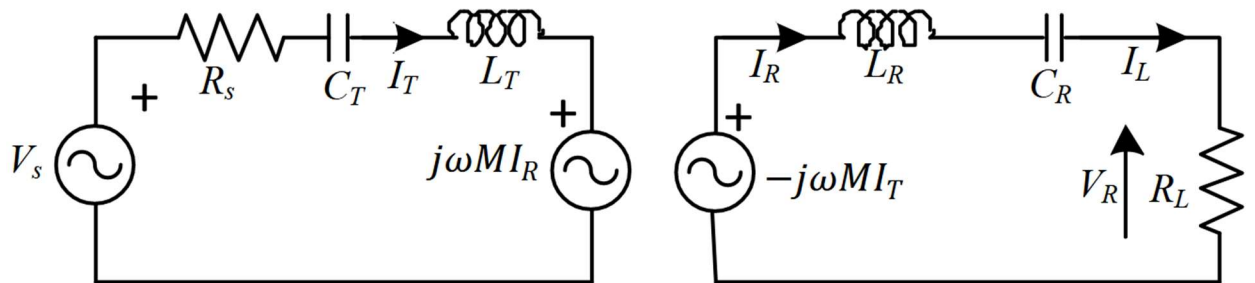


Figure 2. 7 Series-Series Topology

At resonant frequency, Tx and Rx side impedances are minimal and equal to  $R_s$  and  $R_L$  respectively, that is:

$$Z_T = R_s \quad (12)$$

$$Z_R = R_L \quad (13)$$

$Z_T$  and  $Z_R$  are the Tx and Rx side impedances respectively.

The efficiency,  $\eta$  of this topology at resonance is given by,

$$\eta_R = \frac{\omega^2 M^2}{\omega^2 M^2 + R_L R_s} \quad (14)$$

Where  $\omega$ ,  $M$  and  $\eta_R$  are the resonant frequency, mutual inductance between the coils and efficiency at resonance respectively.

### Series-Parallel Topology

This topology allows for efficient power transfer while reducing the voltage across individual coils [9]. The primary compensation is dependent on mutual coupling. For stronger magnetic coupling, the SP resonant inductive link requires a high capacitance value. Peak efficiency obtained using this topology is lower than the SS resonant inductive connection [8].

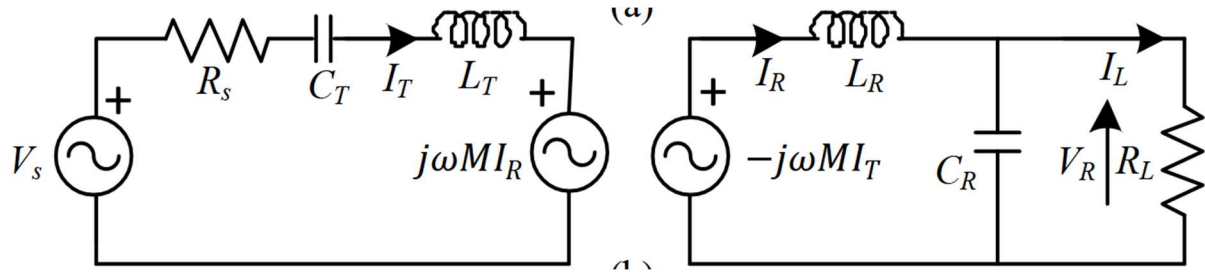


Figure 2. 8 Series-Parallel Topology

### Parallel-Parallel Topology

Suitable for applications where the transmitter and receiver sides have similar voltage requirements [9].

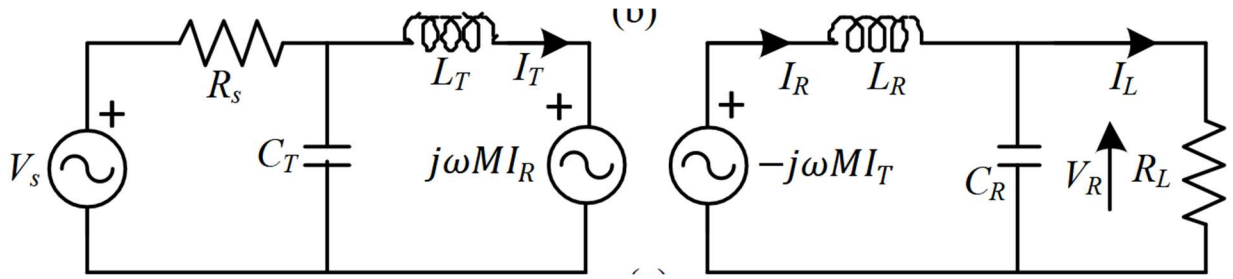


Figure 2. 9 Parallel-Parallel Topology

In [6], a WPT system has been proposed where PP topology is used and to further optimize energy efficiency intermediate coils are added to the system by the location of three or four coils that have the same resonant frequency.

### Parallel-Series

A suitable topology in applications where there is a significant difference in voltage requirements between the transmitter and receiver sides [9]

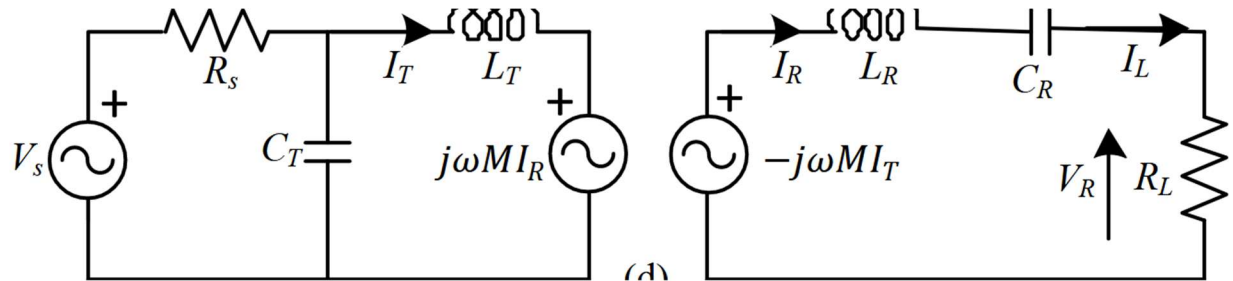


Figure 2. 10 Parallel-Series Topology

A common topology for achieving resonant inductive coupling is the **LCL-LCL Compensation Circuit** which consists of two resonant inductors and two resonant capacitors. The resonant inductors are of the same value matching with the inductors of both coils. This symmetric T-type network has the qualities of [7]:

- i. Voltage-Current conversion
- ii. Impedance transformation

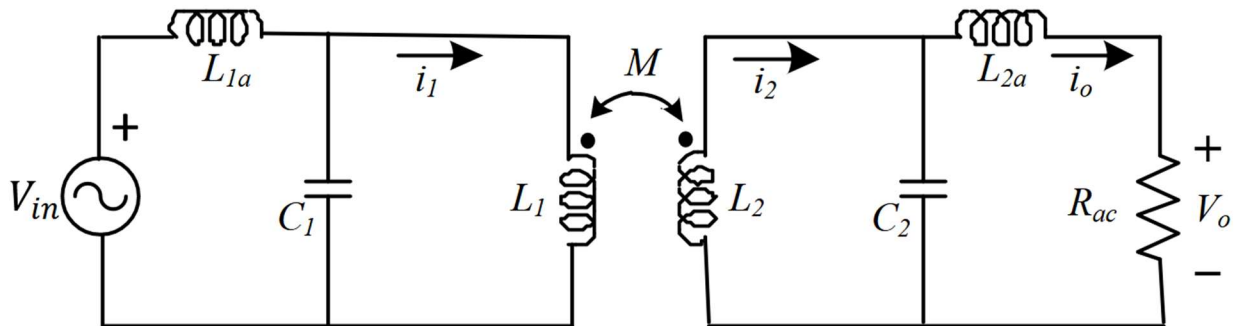


Figure 2. 11 LCL-LCL Compensation Topology

The LCL-LCL topology consists of LCL filters on both Tx and Rx sides contributing to enhanced power transfer efficiency and robustness by ensuring the impedance of the system is well-matched [9]. It operates on the concept of a loosely coupled transformer and mutual inductance model [7]. At the resonance condition, the collapsing magnetic field of the inductor induces an electric current in its windings which charges the capacitor. Subsequently, the discharging capacitor generates an electric current that expands the inductor's magnetic field. In this process, the inductor and capacitor exchange equal amounts of power [7].

[7] proposes an LCL-LCL topology based resonant WPT system for EV charging.

LCL-LCL Topology is a popular choice for resonant inductive WPT systems [9] because of its advantages which include:

- i. Mitigating harmonic distortions
- ii. Improving the power quality of the system by enabling effective filtering and resonance establishment
- iii. Proper voltage stress distribution
- iv. Stability enhancement
- v. Design flexibility

The value of output current for an LCL-LCL topology is independent of load therefore it is possible to maintain a constant load current by maintaining a constant input voltage, resonant frequency and mutual inductance.

## 2.6 Coil Design Optimization for Maximum Efficiency

Methods of wireless power transfer must be as efficient as possible to reduce losses and to deliver the required power [12]. Achieving maximum power transfer efficiency involves geometrically optimizing a coil by employing small ohmic resistance combined with high self-inductance [5]. Coil design is influenced by factors such as available installation space, power transfer capacity of the system and desired efficiency and misalignment tolerance of the coils [9]. Power transfer efficiency is affected by coil size and shape, transmission medium distance and attenuation level and the terminating circuitry of both the Tx and Rx coils [5], [12]. Expanding the air gap between the Tx and Rx coils heightens the need to enhance the quality factor (Q) and coupling coefficient (k) in Tx and Rx coil construction [13]. Quality factor is the ratio of maximum energy stored in the circuit to the energy dissipated in the circuit per cycle of oscillation [10] and is determined by a coil's self-inductance, AC resistance and operating angular frequency ( $Q=\omega L/R_{ac}$ ) [14]. [13] proposes the use of equal-sized coils, expanding coil radii and reducing the air gap length between the Tx and Rx coils as strategies for improving coupling and in return transfer efficiency.

### 2.6.1 Optimizing Coil Structure for Maximum Efficiency

Finding an optimal coil geometry to maximize power transfer efficiency requires exploiting coil self-inductance to yield an ohmic resistance that provides strong coupling between the primary and secondary coils. Coil self-inductance is a factor of number of turns, radius of the coil and length of the coil [5]. In WPT, the primary coil architectures used are helix and spiral designs [9]. Spiral coils are more preferred in most WPT applications [9] because:

- i. They offer more uniform flux density across the coil surface
- ii. The coupling coefficient of spiral coils is about 20% greater than that of helical coils
- iii. They exhibit higher coupling coefficient, k for a given outer diameter and distance separating the Tx and Rx coils

Spiral coils offer versatility in shape with rectangular and circular turns therefore allowing for optimized coil designs [9]. A comparison between the spiral and helix coil structures has been made in Table 2.1

<b>Aspect</b>	<b>Helix Coil</b>	<b>Spiral Coil</b>
Geometrical shape	Helical	Spiral
Inductance	Higher	Lower
Self capacitance	Higher	Lower
Magnetic field orientation	Focused along the axis	Evenly distributed
Physical size	Bulky	Compact
Packaging	Requires more space	PCB friendly

*Table 2. 1 Comparison between the Helix and Spiral Coil Structures*

Coil shapes have been most extensively researched on for low power applications [12]. Coils for ICWPT systems can be classified into three types based on the polarity of the flux distribution [12]. These classifications are:

- i. Unipolar
- ii. Polarized
- iii. Double Polarized

There are four most popular coil structures [12], [13], the circular, rectangular, square and double coils structures. For ICWPT systems, these structures are compared to find the optimum coil shape for the given application.

### **Circular Coils**

Circular coils are of the non-polarized or unipolar flux distribution kind. They have the advantage of having symmetrical flux distribution [12], [13] which is beneficial in applications for inducing uniform fields. The uniform flux distribution results from the symmetrical geometry of the coil. Uniform flux distribution results in uniform coupling and makes the power transferred to be similar in all directions [12]. Uniform power transfer reduces the stress on the power electronic components of the secondary side of the system. When using conductors of low resistance, the number of turns can be increased by reducing the pitch of the coils. The use of ferrite spokes or a ferrite center can significantly increase the coupling between the Tx and Rx coils [12]. The ferrite spoke would act as a low reluctance path for the magnetic field thereby increasing the inductance of the coil and its quality factor, Q. Circular coils ought to be shielded using ferrite materials in

order to protect electronic parts from damage due to flux and to reduce leakage flux [12]. Circular coils provide the best misalignment tolerance [12] and work best when both coils are of the same size.

[12] proposes that the circular coil structure is the optimum coil shape for wireless power transfer. The following parameters of the circular coil are detailed as having an effect on the efficiency of the system:

i. Outer Radius

A larger outer radius as a result in the increase in the number of turns leads to the increase in the self-inductance and hence the Q-factor of the coil. Mutual inductance which is a function of the coupling factor would also increase.

ii. Inner Radius

Inner turns with lower loop radii do not provide significant quality factor improvement as a result of the lower inductance contribution [14].

iii. Pitch

Tightly wound coils with very low pitch between its turns incur low quality factor as a result of the prominence of proximity losses [14].

iv. Number of turns

Inductive coupling increases with an increase in the number of turns. Increasing the number of turns however means longer length of coil wire would be used leading up to an increase in copper losses due to resistance of the wire.

v. Conductor Diameter

Smaller conductor diameters are characterized by more parasitic capacitance in between adjacent turns leading up to the reduction of the quality factor of a coil.

Balance has to be achieved among the various parameters of a circular coil in order to obtain the most optimized coil design for maximum power transfer efficiency of the system since increasing parameters such as the number of turns and coil radii raises coil ohmic resistance despite improving self-inductance [5].

## **Rectangular and Square Coils**

Rectangular and square shaped coils have almost the same structure but differ in performance. These coils have simple designs, are easy to fabricate and have uniform magnetic field distribution along the edges [13]. They a polarized flux distribution [12]. These type of coils have the highest leakage flux [12] and therefore not suitable for efficient wireless power transfer. Since these coils are of the polarized type [12], they offer the highest magnetic coupling compared to other coil shapes but this coupling reduces significantly when the coils are misaligned. To fabricate a rectangular coil of the same area as that of a circular coil, longer wire would be required.

## **Double Coils**

These are two circular coils attached in parallel to each other and have reduced leakage flux and form a polarized flux distribution at the center [12]. This coil structure takes up more space compared to other coil shapes and require a lot more wire to fabricate [12]. Double coils provide better misalignment tolerance and have one-sided flux distribution similar to circular coils and also have the property of reduced leakage flux. For a similar size of double coil and circular coil, the double coil can achieve as much as 1.5 times the magnetic coupling of a circular coil [12].

Often, a coil structure with greater tolerance for distance variation between the Tx and Rx will have decreased tolerance for misalignment [12].

### **2.6.2 Selecting Optimal Coil Materials to Maximize Efficiency**

For maximum efficiency, the coil wire selection should have [5], [12]:

- i. Low AC losses
- ii. Capability to handle high fluctuating currents and voltages
- iii. Low ohmic resistance to yield large intrinsic quality factor of the coil

As frequency of the system is increased, the AC resistance of regular wires also increases due to the skin and proximity effects [10]. The alternative to regular wires is the Litz wire which consists of many thin strands each individually insulated and wound into a wire. In [8], flexible sheet ferrite material is used at the back-side of the wireless power path in order to boost the coupling of the Tx and Rx coils. The increase in mutual inductance between the coils increases the maximum efficiency of the system.

An inductive coupled wireless power transfer system's magnetic coupling efficiency,  $\eta_k$  is given by [3]:

$$\eta_k = \frac{\text{Output power across } R_{eq}}{\text{Output power across } R_{eq} + \text{Power Losses}} \quad (15)$$

Where  $R_{eq}$  is the equivalent load resistance which includes DC load resistance and any other resistive part of the circuit such as the rectifier, voltage regulator etc.

Equation (15) indicates that reduction of the power losses would lead to higher value of the system's magnetic coupling efficiency. One of the ways therefore of optimizing coil design for maximum efficiency is by minimizing coil losses (conduction losses) and core losses (for coils integrated with cores). Coil conduction losses are divided into two categories, DC losses(copper losses) and AC losses(skin and proximity effects) [3]:

### **DC Losses**

When a DC current flows through an inductor, DC losses are the result of current flowing through the wire with resistance  $R$ , power( $I^2R$ ) is dissipated in the form of heat [3]. Increasing the gauge of the wire making up the coils can minimize the DC losses but comes along with extensive increase in cost, size and weight of the overall WPT system [3].

### **Skin Effect**

Skin effect is the restriction of the flow of alternating current to the surface of the conductor [3]. This restriction is caused by the alternating magnetic field that the current itself generates within the conductor. Skin effect leads to the eventual increase in the effective resistance of the conductor as a result of reduced cross section area for current flow [3].

### **Proximity Effect**

When another conductor is brought into proximity to one or more other nearby conductors, such as within a closely wound coil of wire, the distribution of current within the conductor will be constrained to smaller regions. The resulting current crowding is what is called the proximity effect and it increases with frequency [3]. Current crowding results in an increase in the effective resistance of the coil leading to higher power losses. In inductive coils, proximity effect losses dominate over skin effect losses [3]. In Litz wire windings, the proximity effects are classified into

two that is internal proximity effect which is the effect of other currents in the bundle and the external proximity effect which is the effect of current in other bundles.

### **Mitigation of the Proximity and Skin Effects**

Using Litz wire to construct the primary and secondary coupling coils. Each strand of the Litz wire is not thicker than the skin depth which ensures an efficient use of the conductive area. The strands are woven together so that the location of each strand alternates between the center of the wire and the edge of the wire. This ensures that each strand is subjected to the proximity effect in a similar manner and therefore carry the same current. Using Litz wire therefore decreases the AC resistance of the coils considerably [8].

### **Core Losses**

Incorporating flexible ferrite cores in the coil design improves the misalignment tolerance of the coils by creating a path of less reactance for flux flow [8]. Coils integrated with magnetic cores are however accompanied by hysteresis and eddy current losses. Extra system components such as the magnetic cores also increase the weight and cost of the system [8].

All ferromagnetic materials tend to retain some degree of magnetization after exposure to an external magnetic field. Hysteresis is this tendency to stay magnetized. It takes energy to overcome this opposition to change every time the magnetic field produced by the primary coil changes polarity(twice per AC cycle) [3]. Hysteresis losses can be minimized by choosing a core with low hysteresis (thin B-H curve) and designing the core for minimum flux density (large cross-sectional area).

When a low resistivity material is placed in a varying magnetic field, electric currents are induced in the material. These eddy currents must overcome an electrical resistance as they circulate in the core and therefore dissipate heat. Eddy current losses can be minimized in order to maximize efficiency by selecting magnetic core materials that have low electrical conductivity for example ferromagnetic materials such as ferrites [3].

#### **2.6.3 Proposed Coil Design Optimization Methods for Maximum Efficiency**

[15] proposes a novel receiving coil structure where the coil is wound on a drum core with a thin axis. The top and bottom of the drum core have large surface area to effectively collect the

magnetic flux for large mutual inductance. The thin axis reduces the wire length and thereby reducing the parasitic AC resistance of the coil. In the proposed structure, flux lines turn mainly in the magnetic core because the winding edge is covered with the core. The large flux density does not therefore lead to intense magnetic field owing to the high permeability of the core material and induction of eddy currents in the coil wire is thus suppressed.

[11] proposes a three-coil WPT system where parasitic resistances of the coils is minimized by using high quality Litz wire.

[16] proposes an inductive coupled WPT where two identical circular single-loop resonant coils for source and load coils have been used to achieve maximum power transfer.

[17] proposes use of single-loop uniform-sized circular coils

[14] presents guidelines for the design of highly efficient WPT systems with spiral miniature receiver coils and larger transmitter coils. The theoretical maximum power transfer efficiency of the WPT is proposed to be set up when the equivalent load is at its optimum value and is expressed in terms of the quality factors ( $Q$ ) of the Tx and Rx coils and coupling coefficient ( $k$ ).  $Q$  and  $k$  which are dependent on coil parameters and the position of Tx and Rx are identified as the key performance indices for WPT coil design.

[18] proposes the use of flat circular coils for both the Tx and Rx in order to maximize coupling coefficient.

[9] proposes the use of identical spiral coils made of Litz wire as the Tx and Rx

# Chapter 3: DESIGN AND IMPLEMENTATION

## 3.1 System Overview

The wireless power transfer system developed in this project transfers electrical power to low-power devices across an air gap of approximately 40mm using resonant inductive coupling. At its core, the system comprises two magnetically linked sub-assemblies; a series-compensated transmitter and a parallel-compensated receiver; whose tank circuits are both tuned to a common resonant frequency of 100kHz.

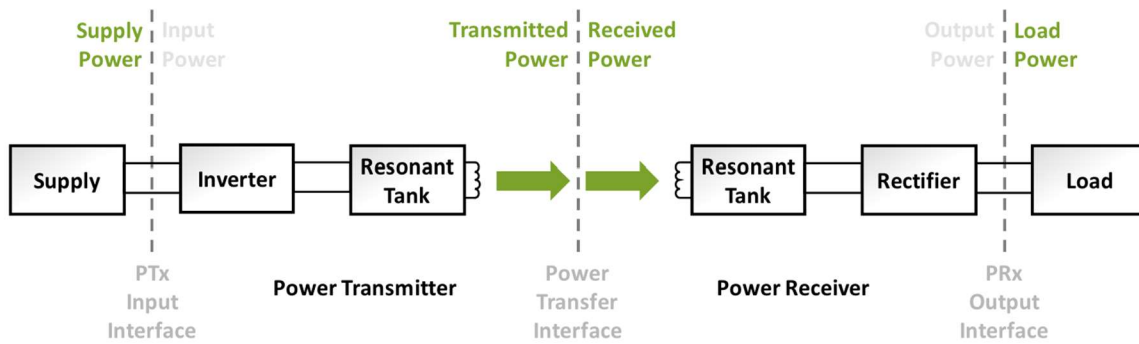


Figure 3. 1 Simplified Model of the WPT System

On the Tx side, a 12V/2A plug-pack feeds a H-bridge inverter built from four IRFZ44N MOSFETs. The inverter is driven in complementary mode by a pair of IR2110 half-bridge gate driver ICs, which in turn receive their logic-level control signals from an Arduino UNO. A buck regulator (LM2596) taps the 12V rail to provide a stable 5V rail for the microcontroller and for the IR2110 logic supplies. The Arduino's firmware configures Timer-1 for phase-correct PWM generation at 100kHz and 50% duty cycle, producing a non-inverted signal on pin9 and its complement on pin10. These two signals ensure that diagonal MOSFET pairs switch alternately, generating an ac square wave that excites the series LC network formed by the Tx coil and its compensation capacitor. Energy couples magnetically across the air gap into the Rx coil, which is shunted by a parallel compensation capacitor so that the Rx tank also resonates at 100kHz. The resulting high circulating current raises the coil voltage, which a Schottky full-bridge rectifier (4; IN5819 diodes) converts to pulsating dc. A bulk electrolytic capacitor smooths this waveform presenting regulated dc output suitable for driving low-power loads such as LED.

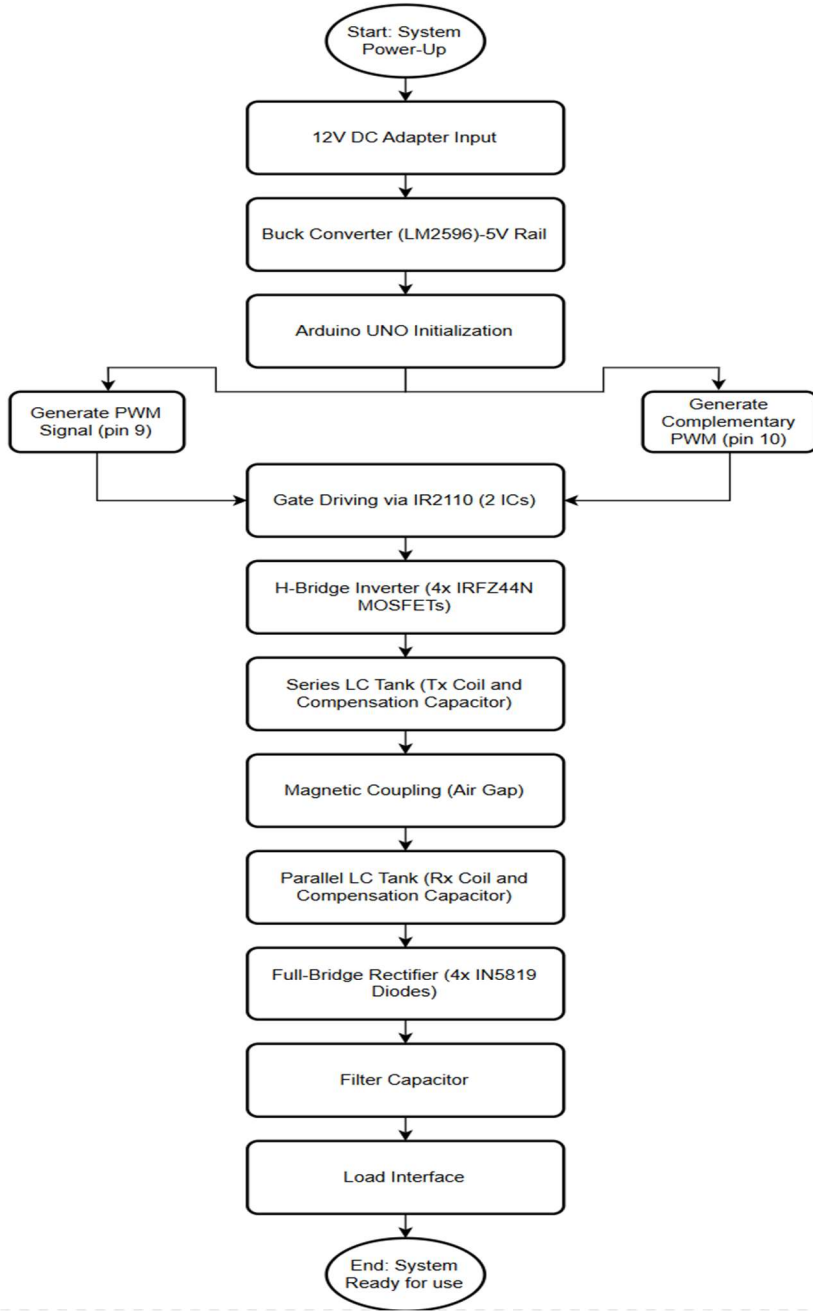


Figure 3. 2 System-level Flowchart

Although this prototype is based on open-loop operation, the modular firmware and clearly partitioned power-stage layout leave scope for future closed-loop enhancements such as load-detected PWM gating without altering the fundamental architecture. Overall, this design balances component availability and efficiency, making it robust for demonstrating resonant inductive power transfer principles.

### 3.2 Design Goals and Requirements

The primary objective of this project is to demonstrate reliable wireless power delivery to low-power devices while preserving constructability, user safety and reasonable component cost. To translate this broad aim into actionable design work, a layered requirements approach has been adopted that distinguishes **electrical performance goals**, **functional requirements** and **practical constraints**.

Requirement Statement	Target Value	Subsystem (s) Responsible
Regulated DC to load	5-8V at 0-200mA ( $\leq 1\text{W}$ )	Receiver LC Tank, rectifier, filter capacitor
End-to-end efficiency	$\geq 40\%$ at 1W into 40mm air-gap	All power stages
Resonant Switching Frequency	100kHz	MCU firmware, Tx/Rx compensation networks
Air-gap operating range	$40\text{mm} \pm 5\text{mm}$	Magnetic links (coils)
Safe touch temperature	$< 45^\circ\text{C}$ on any exposed metal	MOSFETs, rectifier
PWM duty cycle symmetry	50%	Firmware, IR2110 (MOSFET Drivers) Stage

Table 3. 1 Main Design Requirements and Sub-System Responsibility

**Electrical Performance Goals:** Target end-to-end efficiency  $\eta \geq 40\%$  ensures that inverter conduction and switching losses, magnetic link losses, and rectifier drop are all kept within acceptable ranges. Resonant operating frequency of 100kHz balances skin-effect and MOSFET switching-loss considerations against audible noise avoidance and determine the component values convenient for the chosen coil inductances. Voltage and current ratings for every power-stage component are specified within a  $\geq 50\%$  safety margin above anticipated operating stress.

**Functional Requirements:** The system is to deliver steady 5-8V dc across the load for currents up to 200mA, maintain that output over an air gap tolerance of  $40\text{mm} \pm 5\text{mm}$ , and operate reasonably without user tuning. Firmware on the Arduino UNO should initialize power transmission within 500ms of power-on, and should gate-off the PWM stream in the event of detected over-voltage, paving the way for future closed-loop enhancements.

**Practical Constraints:** Cover user safety and mechanical considerations. Touch temperatures on accessible metal surfaces must stay below 45°C and the Tx and Rx module boards fit on medium sized perf boards for the final demonstration. These constraints drove choices such as the use of low-ESR electrolytics to curb thermal rise.

### 3.3 Theory of Resonant Inductive Coupling

WPT using resonant inductive coupling is fundamentally based on the efficient exchange of energy between two magnetically coupled resonators. Each resonator consists of an inductor and a capacitor, forming an LC tank that naturally oscillates at a frequency determined by the values of L and C. When these two tanks are tuned to the same resonant frequency and are positioned in proximity, energy is transferred from one to the other. This section presents the essential concepts necessary for designing such a system.

#### 3.3.1 Resonant Frequency

Resonance in an LC circuit occurs when the inductive and capacitive reactances are equal in magnitude but opposite in phase, causing them to cancel each other out. At this condition, the impedance of the circuit is purely resistive, and the voltage and current in the tank are in phase. This leads to a significant increase in circulating current, which in turn enhances the energy exchange between the magnetic fields of the Tx and Rx coils. The resonant frequency,  $f_0$  of an LC circuit is given by the expression:

$$f_0 = \frac{1}{2\pi\sqrt{LC}} \quad (3.1)$$

In this project, the Tx and Rx coils are estimated to have self-inductances of approximately 80 $\mu$ H. Based on this inductance value, and the system design requirement of operating at a frequency of 100kHz, the necessary capacitance to achieve resonance has been calculated using equation (3.1). The resulting value is 33nF for both the Tx and Rx coils.

Environmental factors such as temperature changes, coil alignment, and variation in the permeability of the ferrite plates can affect the exact resonant frequency. Use of stable capacitors and fixed-frequency PWM generation helps reduce the impact of these shifts.

### 3.3.2 Quality Factor and Link Efficiency

While resonance determines when energy is most efficiently transferred, the quality factor, Q, determines how well power transfer occurs. The Q factor of an LC circuit is a measure of its energy retention capability (it compares the energy stored in the tank to the energy dissipated per cycle). A higher Q means lower resistive losses and a sharper resonance peak, which is favorable for efficient WPT. Q is calculated using the formula:

$$Q = \frac{\omega_0 L}{R_{equiv}} \quad (3.2)$$

Where  $\omega_0=2\pi f_0$  and  $R_{equiv}$  represents the equivalent series resistance (ESR) in the tank, accounting for coil resistance, core losses, and any load reflected back into the transmitter side.

In this project, both the Tx and Rx coils are standardized A11 wireless charging coils.

For the Tx coil, for ac resistance  $R_{ac}$ ,  $L \approx 80\mu H$  and  $f_0=100kHz$ , the resulting Q is approximately:

$$Q_{TX} \approx \frac{2\pi \times (100000) \times 80 \times 10^{-6}}{R_{ac}} \quad (3.3)$$

For the Rx, the effective resistance is influenced heavily by the connected load and the internal losses in the rectifier and smoothing capacitor. For equivalent series resistance (ESR) including reflected load resistance, and  $L \approx 80\mu H$ , the Q factor is:

$$Q_{RX} \approx \frac{2\pi \times (100000) \times 80 \times 10^{-6}}{ESR} \quad (3.4)$$

These values represent a balance: increasing Q generally improves efficiency but narrows the bandwidth, making the system more sensitive to detuning. Given the open-loop nature of this project build, overly narrow resonance peaks would lead to erratic power delivery on variation of environmental conditions. The selected Q values thus ensure reliable operation without excessive tuning complexity.

To estimate how efficiently the system transfers power at resonance, the following approximate formula is used for loosely coupled systems

$$\eta \approx \frac{k^2 Q_{TX} Q_{RX}}{(1 + \sqrt{1 + k^2} Q_{TX} Q_{RX})^2} \quad (3.5)$$

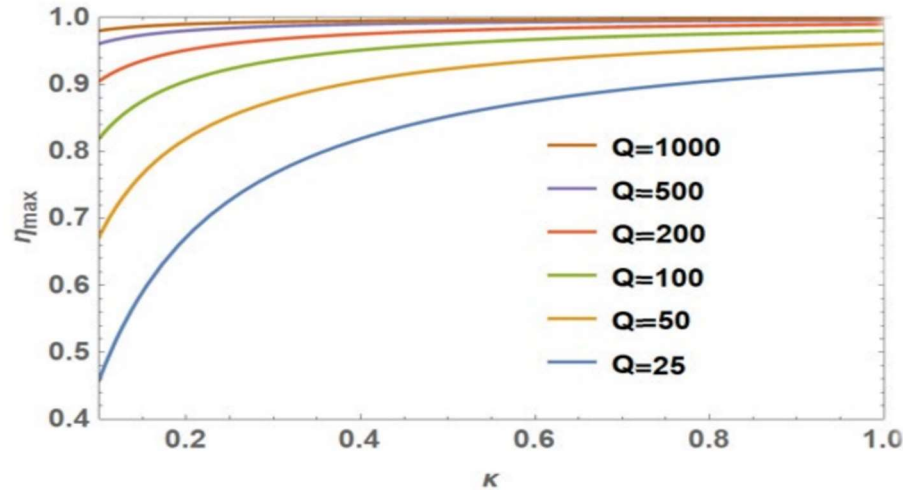


Figure 3. 3 Graph of Efficiency vs.  $k$  plotted for various  $Q$

### 3.4 Transmitter Sub-System

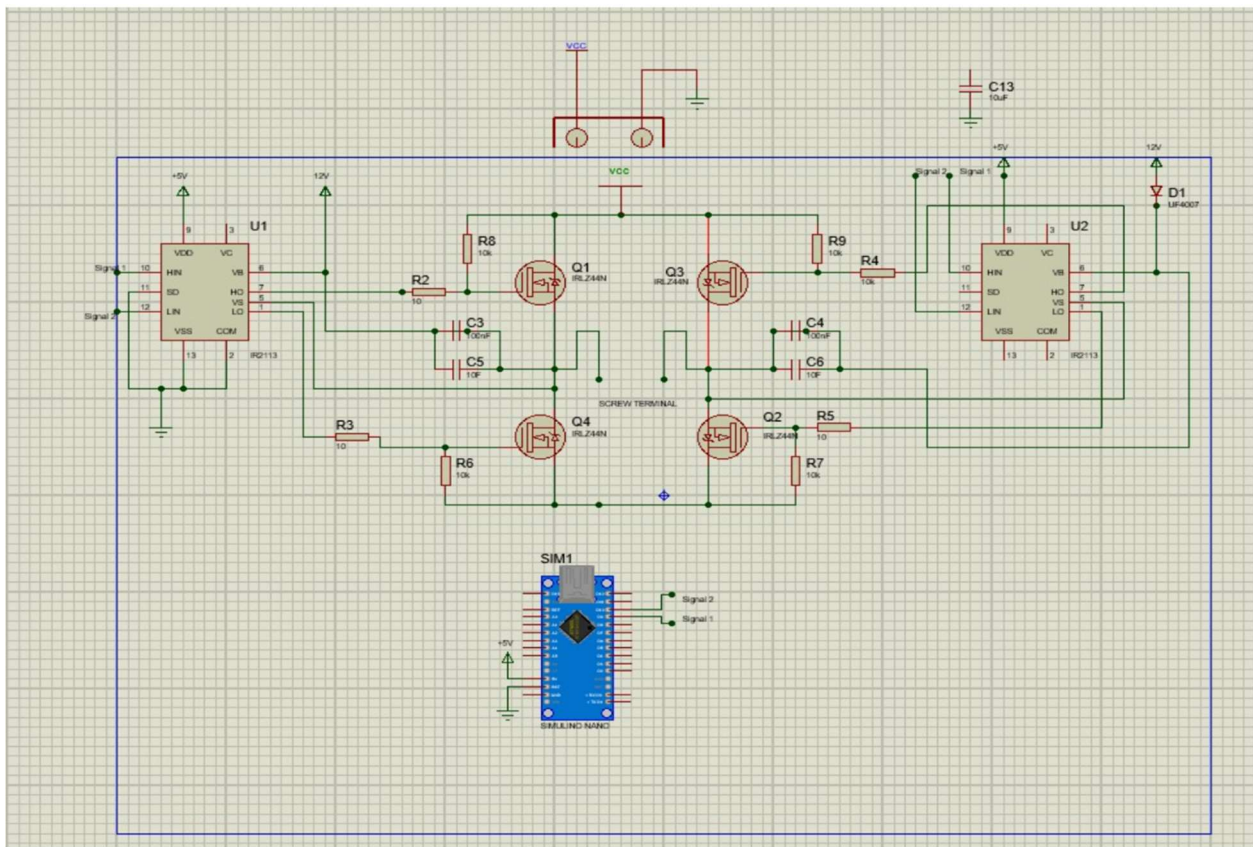


Figure 3. 4 Transmitter Sub-System Schematic

### 3.4.1 Power Supply Rails

The transmitter section of the WPT system requires two distinct supply voltages to serve its high-power and logic-level components: a 12V rail for the inverter stage and gate drivers, and a 5V rail for the Arduino UNO and the logic supply pins of the IR2110 gate driver ICs. Both rails are derived from a common source – a 12V, 2A DC adapter connected to mains. The 12V rail directly powers the H-bridge inverter, which is the core of the signal-generation stage in the transmitter. This rail must be capable of supplying sufficient current to drive the MOSFETs and handle the reactive load imposed by the series LC tank during resonant operation. The 2A rating provides comfortable headroom. In addition to powering the H-bridge, the same rail supplies the high-side bootstrap circuitry for the IR2110 gate drivers, which rely on the 12V source to maintain sufficient gate drive voltage for the high-side MOSFETs.

In order to accommodate the 5V logic requirements of the Arduino UNO and the IR2110s' low-side logic supply pins, a buck converter module based on the LM2596 is used. The LM2596 is a step-down switching regulator well-suited for this application due to its compact module form, high efficiency, and ease of configuration. It provides a stable 5V output from the 12V input with minimal power loss, ensuring both thermal efficiency and reliability. The decision to use an LM2596-based buck converter instead of a linear regulator such as the LM7805 was driven by efficiency and heat dissipation considerations. Bulk electrolytic capacitors and  $0.1\mu F$  ceramic decoupling capacitors are placed close to the LM2596 module to smooth out voltage transients and reduce ripple. These support both startup stability and the transient response during changes in switching load caused by the dynamic operation of the inverter.

Rail	Voltage (V)	Max Current (A)	Feeds	Source Component
12V Rail	12.0	2.0	H-Bridge Inverter, IR2110 high-side bootstrap	12V/2A DC Adapter
5V Rail	5.0	~0.3	Arduino, IR2110 logic supply	LM2596 Buck Converter

Table 3. 2 Power Rails Specifications

The power supply architecture ensures that each subsystem receives clean and appropriately regulated voltage while maintaining overall system efficiency and thermal safety. It serves as the

backbone of the transmitter design, enabling stable PWM signal generation, effective MOSFET switching, and ultimately reliable power transmission to the receiver side.

### 3.4.2 PWM Generation (Arduino UNO)

At the heart of the transmitter's switching stage is the Arduino UNO, which is responsible for generating the two key control signals required by the gate driver ICs (IR2110) that manage the H-bridge MOSFETs. These control signals must be carefully timed, consistent in frequency and duty cycle, and complementary to ensure proper alternating operation of the inverter's diagonal MOSFET pairs. Arduino UNO meets these needs through hardware-based PWM generation on two of its digital output pins. The chosen configuration uses Timer1, a 16-bit timer built into the ATmega328P microcontroller, which allows for precise control over the PWM waveform. This timer is configured to operate in Phase Correct PWM mode, which offers a symmetrical output waveform around the timer's top value (ICR1), helping maintain a consistent 50% duty cycle. This mode is well-suited for resonant applications where switching symmetry helps reduce switching losses and EMI.

The UNO outputs the non-inverted PWM signal on digital pin9 (OC1A) and the complementary inverted signal on digital pin10 (OC1B). The complementary nature ensures that only one diagonal MOSFET pair in the H-bridge is active at any given time, which is essential for preventing shoot-through (simultaneous conduction of both high-side and low-side switches on one leg). The PWM frequency is set at 100kHz in line with the resonant frequency of the LC tanks. This frequency is achieved by configuring the timer with the appropriate top value using the Input Capture Register (ICR1). Since the UNO's system clock is 16MHz, setting ICR1=79 results in a timer overflow rate that produces a 100kHz waveform:

$$f_{PWM} = \frac{f_{clk}}{2 \times ICR1} = \frac{16MHz}{2 \times 80} = 100kHz \quad (3.6)$$

```

void setup()
{
    // Set pin 9 and pin 10 as outputs
    pinMode(9, OUTPUT); // OC1A
    pinMode(10, OUTPUT); // OC1B

    // Clear control registers
    TCCR1A = 0;
    TCCR1B = 0;

    // Set Fast PWM mode with ICR1 as TOP => WGM13=1, WGM12=1, WGM11=1, WGM10=0 (Mode 14)
    TCCR1A |= (1 << WGM11);
    TCCR1B |= (1 << WGM12) | (1 << WGM13);

    // Set Compare Output modes:
    // - OC1A in Non-inverting mode => COM1A1=1, COM1A0=0
    // - OC1B in Inverting mode => COM1B1=1, COM1B0=1
    TCCR1A |= (1 << COM1A1); // Non-inverting on OC1A
    TCCR1A |= (1 << COM1B1) | (1 << COM1B0); // Inverting on OC1B

    // Set TOP and Compare registers
    ICR1 = 159; // TOP for 100kHz
    OCR1A = 80; // 50% duty on channel A
    OCR1B = 80; // 50% duty on channel B

    // Prescaler = 1 => CS10=1
    TCCR1B |= (1 << CS10);
}

```

*Figure 3. 5 Arduino code showing Timer1 configuration for 100kHz complementary PWM generation*

To prevent inverter cross-conduction during switching transitions, the IR2110 gate drivers introduce a built-in dead time of approximately 12ns. This delay ensures that one MOSFET fully turns off before its complementary device turns on, minimizing the risk of high-current faults. While the Arduino UNO itself cannot directly generate dead-time between its output, the inclusion of the IR2110s with internal non-overlap handling makes it possible to use standard complementary signals safely. The PWM generation strategy is simple yet effective, enabling robust inverter control using minimal hardware.

### 3.4.3 Gate Driver Stage (IR2110)

The PWM signals generated by the Arduino UNO are not capable of directly switching the power MOSFETs in the H-bridge inverter. The microcontroller outputs are limited to 5V logic levels and can only source or sink a few tens of milliamperes, which is insufficient for rapidly charging and discharging the relatively large gate capacitances of the inverter MOSFETs. To bridge this gap, the system employs two IR2110 high-voltage, high-speed MOSFET gate driver ICs (one for each half-bridge leg of the inverter). The IR2110 is a dual-channel driver capable of operating one high-side and one low-side MOSFET. It supports gate drive voltage up to 20V, fast rise/fall times, and features internal shoot-through protection through a built-in non-overlapping control logic. Each

IR2110 receives two logic signals: one from Arduino pin9 (signal 1), and the other its inverted counterpart from pin10 (signal 2). These logic inputs control the output pins HO (high-side output) and LO (low-side output), which are connected to the gates of the respective MOSFETs in the inverter.

One of the most critical aspects of using the IR2110 is managing its high-side gate drive, which requires a floating voltage source that is referenced to the switching node VS. This is achieved using a bootstrap circuit consisting of a fast recovery diode (UF4007) and a ceramic capacitor (100nF) connected between pins VB and VS. During the low-side conduction phase, the bootstrap capacitor charges up from the 12V rail. Then, when the high-side switch is turned on, this stored charge acts as a temporary floating supply, lifting the gate above the source to turn the high-side MOSFET fully on. The low-side gate drive (LO) is simpler, as it is referenced directly to ground, and can be driven from the 12V supply via the V<sub>CC</sub> pin of the IR2110.

Dead-time insertion is another key advantage of using the IR2110. While the Arduino generates complementary PWM signals, the IR2110 introduces an internal non-overlap period (typically 12ns) which ensures that the high-side and low-side MOSFETs on the same leg are never on at the same time. This protection is vital to prevent shoot-through currents, which could otherwise damage the MOSFETs or the power supply.

<b>Parameter</b>	<b>Value/Feature</b>	<b>Rationale for use in the system</b>
V <sub>CC</sub> Supply Voltage	10-20V	Compatible with 12V rail used for gate driving
Gate Drive Output Current	±2A	Adequate for driving IRFZ44N gates quickly at 100kHz
Bootstrap Capability	Yes	Allows high-side N-channel MOSFET switching using floating driver
Input Logic Compatibility	TTL/CMOS (3-15V)	Fully compatible with Arduino UNO 5V PWM outputs
Propagation Delay	~120ns	Acceptable delay for 100kHz operation; ensures predictable timing
Rise/Fall Time	<100ns	Enables fast transitions to reduce switching loss

Dead-time Handling	Internal non-overlap logic	Prevents shoot-through without complex MCU timing schemes
Package	DIP-14	Allows easy prototyping on perf-board

Table 3. 3 Key IR2110 Specifications and Rationale for Use

Using two IR2110 (one per inverter leg), ensures that both sides of the H-bridge receive reliable and isolated gate control, enabling the system to generate a balanced AC waveform across the Tx coil.

#### 3.4.4 H-Bridge Inverter

The H-bridge inverter is the functional core of the transmitter's power conversion stage. It is responsible for transforming the regulated 12V DC input into a high-frequency (100kHz) square-wave AC signal, which is used to excite the resonant LC tank connected to the Tx coil. This square-wave approximates the sinusoidal excitation needed for resonant energy transfer and is suitable for driving the inductive load, especially given the filtering effect of the tank circuit. The inverter is constructed using four IRFZ44N N-channel MOSFETs in a full H-bridge configuration. Each diagonal pair of MOSFETs is controlled by a separate IR2110 gate driver, which receives complementary PWM signals from the Arduino UNO.

During operation, each PWM cycle alternately turns on opposing diagonal MOSFET pairs (for example, Q1 and Q2, then Q3 and Q4). This creates an alternating polarity voltage across the LC tank, centered around ground. Because the output is a 100kHz square wave, and the tank is resonant at the same frequency, the circuit normally filters higher harmonics, allowing primarily the fundamental to excite the Tx coil efficiently.

The IRFZ44N is a commonly available, low-cost, and reliable N-channel MOSFET that suits the inverter's low-voltage, moderate-current design requirements. Key parameters include:

- i.  $V_{DS(\max)} = 55V$ : Sufficient for handling switching spikes on a 12V rail with safety margin
- ii.  $I_D \sim 49A$  at  $25^\circ C$ : Far exceeding actual load current
- iii.  $R_{DS(on)} = 17m\Omega$ : Low conduction loss
- iv.  $Q_g$  (Total Gate Charge) =  $67nC$ : Manageable with IR2110 drivers at 100kHz

Parameter	Value	Relevance to Design
Drain-Source Voltage, V <sub>DS</sub>	55V	Provides safe headroom over 12V, including switching transients
Continuous Drain Current, I <sub>D</sub>	49A at 25°C	Far exceeds expected current (~1A max); strong thermal margin
On-State Resistance, R <sub>DS(on)</sub>	17mΩ at V <sub>GS</sub> =10V	Low conduction loss during switching; minimizes heat dissipation
Total Gate Charge, Q <sub>g</sub>	67nC	Manageable gate drive requirements at 100kHz with IR2110
Gate Threshold voltage, V <sub>GS(th)</sub>	2.0 – 4.0V	Ensures turn-off at low logic levels; suitable for 12V gate drive

Table 3. 4 Electrical Characteristics of IRFZ44N

Each MOSFET experiences two primary types of loss, that is, **conduction loss** and **switching loss**. Conduction loss occurs when a MOSFET is on, and is estimated as:

$$P_{cond} = I^2 \times R_{DS(on)} \quad (3.7)$$

Switching losses occur during transitions and are estimated by:

$$P_{sw} = \frac{1}{2} V_{DS} \times I_D \times (t_r + t_f) \times f_s \quad (3.8)$$

Where t<sub>r</sub>, t<sub>f</sub> and f<sub>s</sub> are rise time, fall time and switching frequency respectively

To protect the MOSFETs from voltage overshoot caused by parasitic inductance, the design includes gate resistors (10Ω) to limit inrush current during switching. Connections for gate drive signals are kept short and routed away from high-current paths to minimize coupling and ringing.

The H-bridge inverter, built using four IRFZ44N MOSFETs, provides a compact and efficient mechanism for generating high-frequency AC. Its performance is enhanced through proper gate driving, proper layout, and protection components, forming a reliable interface between the control logic and the resonant transmitter stage.

### 3.4.5 Series-Compensated Transmitter Tank

The final stage in the transmitter subsystem is the series-compensated LC tank, which plays a central role in enabling efficient resonant inductive power transfer. This stage shapes the square-

wave signal from the inverter into a high-frequency alternating current that drives the magnetic field linking the transmitter to the receiver.

In a series LC configuration, the inductor (Tx coil) and compensation capacitor are connected in series to one another. At the resonant frequency, the inductive reactance and capacitive reactance cancel each other out, minimizing the tank's impedance. This allows for the maximum current to flow through the coil with minimal voltage drop, creating a strong alternating magnetic field at the operating frequency of 100kHz.

The transmitter coil is estimated to have an inductance of approximately 80 $\mu$ H. To tune this coil to resonate at 100kHz, the appropriate series capacitance  $C_{TX}$  is calculated using the resonance formula:

$$f_0 = \frac{1}{2\pi \times \sqrt{L_{TX}C_{TX}}} \quad (3.9)$$

Solving for  $C_{TX}$  gives:

$$C_{TX} = \frac{1}{(2\pi f_0)^2 L_{TX}} \approx \frac{1}{(2\pi \times 100 \times 10^3)^2 \times 80 \times 10^{-6}} \approx 33nF \quad (3.10)$$

A 33nF polypropylene film capacitor is selected, offering excellent frequency stability and minimal drift with temperature thus ensuring consistent performance even during prolonged operation.

The series LC circuit presents minimal impedance at resonance, causing current through the coil to increase significantly even with modest applied voltage. Using 12V supply and negligible total reactance, the peak current  $I_{TX,pk}$  through the coil is estimated by:

$$I_{TX,pk} = \frac{V_{peak}}{X_L} = \frac{12}{2\pi f_0 L} \approx \frac{12}{2\pi \times 100 \times 10^3 \times 80 \times 10^{-6}} \quad (3.11)$$

This circulating current generates the magnetic flux that couples energy to the receiver. The use of Litz wire in the coil helps to minimize skin-effect losses at high frequency, maintaining low coil resistance and supporting a higher Q factor.

The compensation capacitor is placed as close as possible to the coil terminals to minimize parasitic inductance. The capacitor is rated 100V to accommodate possible transient spikes during

switching. The capacitor leads are also kept short to preserve the tanks quality factor. The magnetic field generated by the tank is directed toward the Rx coil and is shaped by a ferrite plate placed at the back of the coil. This ferrite layer increases the coil's inductance slightly and helps focus the field toward the Rx coil, improving the coupling coefficient,  $k$ , and reducing leakage into surrounding components.

Because the capacitor and coil are part of a resonant circuit and not directly supplying power to load, they experience high circulating current but relatively low power dissipation. Nonetheless, they are specified for low ESR and high-frequency operation to prevent heating.

### 3.5 Receiver Sub-System

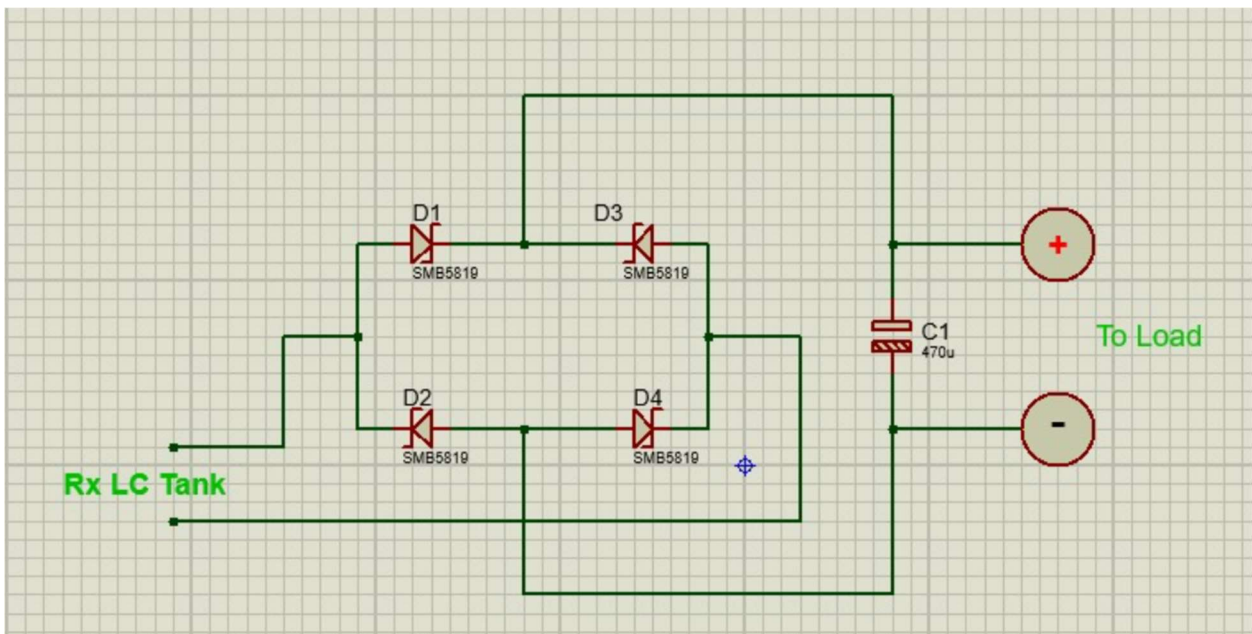


Figure 3. 6 Receiver Sub-System Schematic

#### 3.5.1 Parallel-Compensated LC

On the receiver side of the WPT system, the LC circuit is arranged in a parallel configuration, forming a parallel-tuned resonant tank. While the transmitter tank is optimized to maximize current for strong magnetic field generation, the receiver tank is tuned to maximize voltage across its terminals, which is beneficial since the goal is to supply power to a rectifier and ultimately drive a DC load. At resonance, this parallel arrangement produces a high-impedance condition, where the input current is minimized but the voltage across the tank peaks significantly. This high voltage across the coil enhances the effectiveness of the rectifier stage. The high-impedance nature of the

parallel tank at resonance means that most of the voltage induced by the transmitter's magnetic field appears across the compensation capacitor and Rx coil. This is ideal for maximizing the voltage input to the full-bridge diode rectifier stage, which requires sufficient forward-bias to conduct effectively, since Schottky diodes begin conducting around 0.3-0.4V each.

The Rx coil is estimated to have an inductance of approximately  $80\mu\text{H}$ . To achieve resonance at the system frequency of  $100\text{kHz}$ , the parallel compensation capacitance is calculated using the resonance condition:

$$C_{RX} = \frac{1}{(2\pi f_0)^2 L_{RX}} \approx \frac{1}{(2\pi \times 100 \times 10^3)^2 \times 80 \times 10^{-6}} \approx 33nF \quad (3.12)$$

The parallel tuned LC tank also helps isolate the load from minor detuning effects caused by alignment drift or small coil separation changes. By stabilizing the voltage across the tank, the system ensures that the output voltage remains within the desired range (5-8V DC) even as coupling conditions fluctuate slightly during operation.

The capacitor is placed close to the coil terminals with short lead lengths to minimize parasitic inductance. It is rated 100V ensuring safe operation even under open-circuit or light-load conditions where the tank voltage may rise significantly due to the high Q factor of the Rx coil.

### 3.5.2 Rectifier and Filter

Once the high-frequency AC voltage is induced and boosted by the parallel-resonant Rx tank, it is converted into a stable DC voltage suitable for powering low-power loads. This is accomplished using a full-bridge rectifier followed by a smoothing filter capacitor, forming the final stage in the Rx power path. The AC signal generated across the Rx tank terminals (resonating at  $100\text{kHz}$ ) is fed into a diode bridge rectifier. The bridge is constructed using four IN5819 Schottky diodes, selected for their low voltage drop (0.3-0.4V) and fast recovery characteristics. At high frequencies such as  $100\text{kHz}$ , conventional silicon diodes would suffer from excessive switching losses and poor efficiency. In contrast, Schottky diodes minimize conduction and switching losses, improving the overall efficiency of the rectification process.

The full-bridge configuration ensures that both halves of the AC waveform are utilized, maximizing the energy conversion. During each half-cycle, two diodes conduct while the other two are reverse-biased, directing current to flow through the load in a single direction. The

resulting waveform is pulsating DC, with a peak value close to the amplitude of the received AC signal, minus two diode drops ( $\sim 0.6\text{-}0.8\text{V}$  total). At the output of the rectifier is a  $470\mu\text{F}$  electrolytic capacitor rated at 25V to smooth out the voltage ripple. This capacitor absorbs the pulsating nature of the rectified waveform and provides a continuous DC voltage to the load.

Although the Schottky diodes operate efficiently, they still dissipate heat under load. For a  $100\text{mA}$  load and a total voltage drop of  $0.7\text{V}$  across two diodes conducting in each cycle, the total conduction loss is:

$$P_{rect} = V_{fwd} \times I_{load} \approx 0.7 \times 0.1 = 70\text{mW} \quad (3.13)$$

Each diode thus dissipates roughly  $35\text{mW}$ , which remains well within safe operating limits.

### 3.5.3 Load Interface

The rectified and filtered DC output is delivered to an end-use device. This section of the system must ensure compatibility between the power output characteristics of the receiver and the electrical needs of the connected load while maintaining stable operation even under varying load conditions. In this prototype, load is represented by a low-power LED module that draws approximately  $20\text{-}30\text{mA}$  at a forward voltage of about  $2\text{V}$ . A series resistor is used to limit current through the LED and it is selected based on the measured output voltage of the receiver.

$$R = \frac{V_{OUT} - V_{LED}}{I_{LED}} \quad (3.14)$$

The connected LED provides indication of system operation and serves as a proof-of-concept load that demonstrates successful power transfer. While an LED has been used to demonstrate system operation, the receiver is designed to accommodate a broader range of low-power DC loads. These may include:

- i. Microcontrollers
- ii. Sensor modules (temperature, motion detectors etc.)
- iii. Low-power wireless communication modules such as Bluetooth

## 3.6 Component Selection Justification

A fundamental aspect of engineering design is choosing components that not only meet performance criteria but also align with the project's cost, efficiency, availability and reliability

goals. Table summarizes the major components used in this WPT system, alongside their roles, specification, and rationale for selection.

<b>Component</b>	<b>Role in System</b>	<b>Part No./Spec</b>	<b>Justification</b>	<b>Alternatives Considered</b>
Microcontroller	Generate Complementary PWM Signals	Arduino UNO	Simple setup, accessible Timer1 hardware PWM, USB programming	ESP32, STM32 – more advanced but overly complex for this application
Gate Driver	Drive high and low-side MOSFETs	IR2110	High voltage support, bootstrap circuit, fast rise/fall times	IRS2003 – less available
MOSFETs	Form H-bridge inverter for 12V square wave	IRFZ44N (55V,49A, $R_{DS(on)}=17m\Omega$ )	Low cost, adequate voltage and current ratings	IRLZ44N – similar, but IRFZ44N is more available locally
Compensation Capacitors	Achieve resonance at 100kHz	33nF ceramic	Temperature stable dielectric, low ESR, high frequency tolerance	Electrolytic capacitors – unsuitable for high frequency
Rectifier Diodes	Convert AC to DC	IN5819 (Schottky, 40V, 1A)	Low forward voltage, low conduction loss, fast switching	IN4007 – too slow

Filter Capacitor	Smooth rectified voltage	470µF, 25V electrolytic	Provides sufficient energy storage to reduce ripple, low cost	Film capacitors – too bulky
Buck Regulator	Derive 5V rail from 12V supply	LM2596 Module	Efficient, provides $\geq 2A$ , low heat dissipation vs linear regulator	LM7805 - inefficient

*Table 3. 5 Main Component Choices with Justification*

# Chapter 4: RESULTS AND ANALYSIS

## 4.1 Circuit Realization and Test Setup

The full wireless power transfer (WPT) system was constructed and tested on a breadboard to validate real-world functionality prior to soldering on a perf-board. Unlike simulations, physical testing helps expose the influence of parasitic elements, imperfect alignments, and real-world component tolerances on system behavior. Most components used, such as diodes, capacitors, and MOSFETs match those selected during the design process, except for the coils, which have been manually wound for this prototype.

Due to the absence of an inductance meter, the inductance of each hand-wound coil has been estimated using an online calculator based on coil geometry and turn count. The calculated inductance is approximately  $80 \mu\text{H}$  per coil. These coils have been wound using enameled copper wire. Although this approach introduces slight uncertainty due to spacing variations, it is deemed sufficient for prototype-level testing and resonance tuning within acceptable margins.

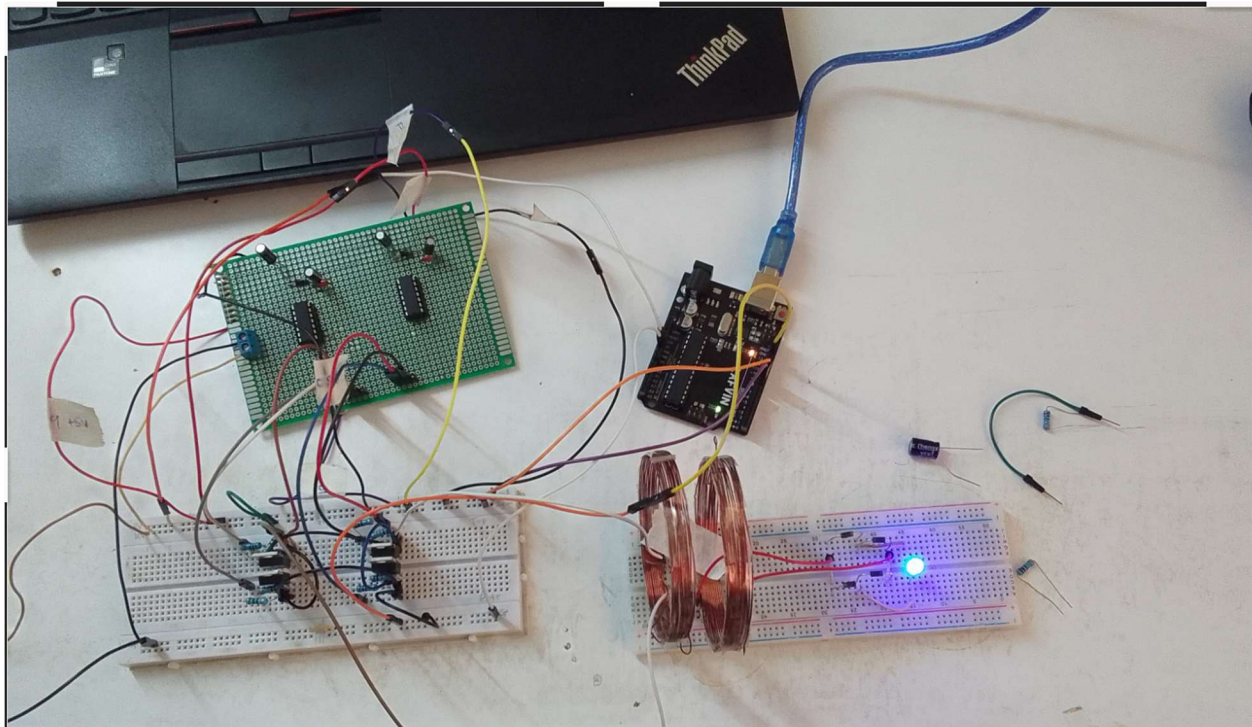


Figure 4. 1 Experimental Setup of the WPT System

The inductance of a coil is highly sensitive to winding tightness, number of turns, coil diameter, and the presence or absence of a magnetic core. In this case, the lack of ferrite cores may have

slightly increased parasitic effects, but resonance is still achievable through compensation capacitor tuning. The hand-wound coil setup has been used to explore how physical and electrical parameters affect system performance. The following key factors have been considered:

- i. The angular orientation between the transmitter and receiver coils,  $\theta$
- ii. The air-gap distance between the two coils,  $d$

These parameters strongly influence mutual inductance ( $M$ ) and coupling coefficient ( $k$ ), both of which govern the efficiency of magnetic energy transfer.

The next section presents the experimental results from this setup and evaluates how these factors impact output voltage obtained on the receiver section.

## 4.2 Effect of Coil Orientation on Power Transfer

This experiment is conducted to determine the optimal angular alignment between the transmitter and receiver coils for maximum power transfer. Since magnetic coupling is highly dependent on the relative orientation of the coils, the receiver coil is tested at three distinct angular positions with respect to the transmitter coil:

- i.  $\theta_1 = 0^\circ$  – Receiver coil directly faces the transmitter coil (perfect axial alignment)
- ii.  $\theta_2 = 45^\circ$  – Receiver coil is tilted at  $45^\circ$  relative to the transmitter coil
- iii.  $\theta_3 = 90^\circ$  – Receiver coil is perpendicular to the transmitter coil axis (orthogonal misalignment)

The input supply voltage is fixed at 12 V DC, and both coils are almost identical in geometry and inductance, estimated at  $80 \mu\text{H}$ . The primary goal is to observe how changes in angular alignment influence the voltage induced across the receiver output.

Supply Voltage (V)	Coil Angle ( $\theta$ )	Output Voltage (V)
12	$0^\circ$	4.02
12	$45^\circ$	2.34
12	$90^\circ$	2.28

Table 4. 1 Receiver Output Voltage at Different Coil Orientations

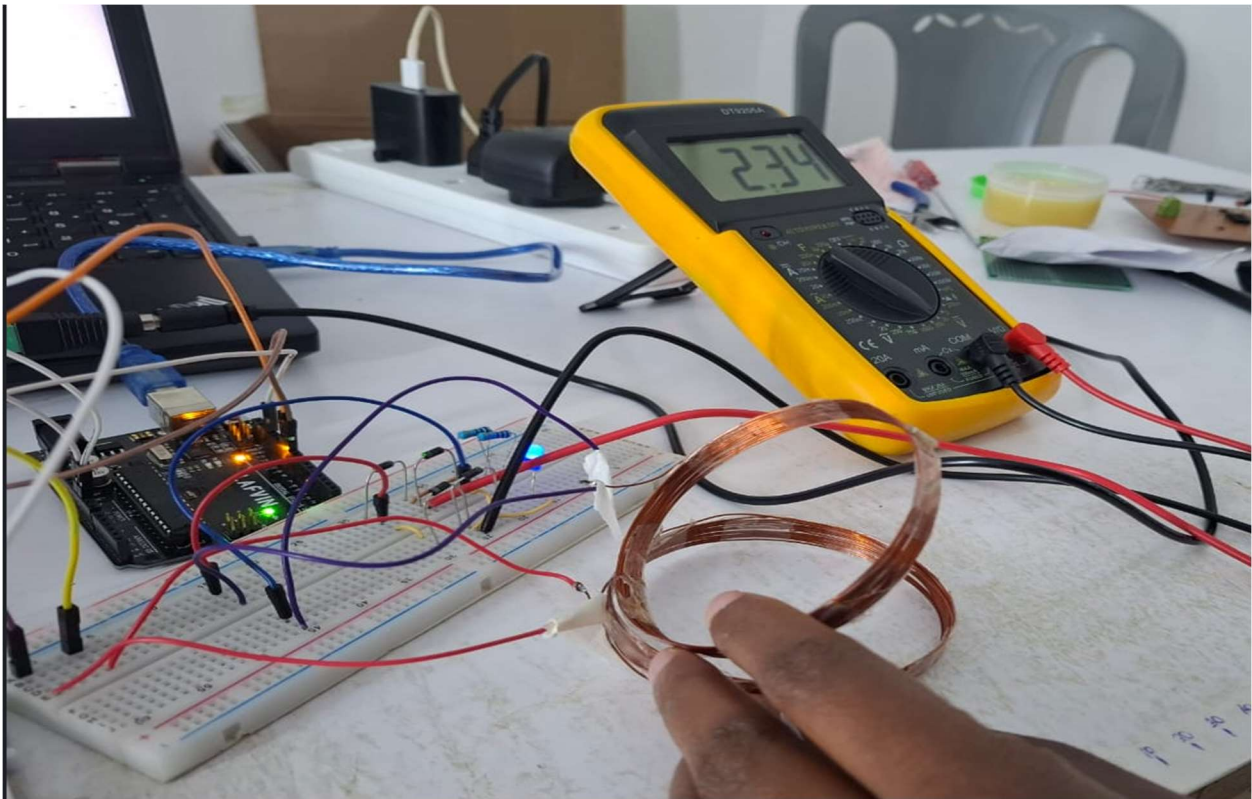


Figure 4. 2 Coils placed at 45 degrees

From the results, it is evident that coil orientation significantly impacts the induced voltage at the receiver. When the coils are perfectly aligned ( $\theta = 0^\circ$ ), the system achieves the highest output voltage, indicating maximum magnetic coupling. At  $45^\circ$ , the output voltage drops, and at  $90^\circ$ , the induced voltage is minimal, demonstrating severely degraded coupling due to the orthogonal field orientation.

These results are consistent with the theoretical understanding of mutual inductance, which is maximized when the magnetic axes of the coils are aligned and minimized when they are perpendicular. The substantial drop in voltage at  $90^\circ$  confirms that magnetic flux linkage is severely reduced in this orientation.

Based on these findings, it is concluded that optimal performance is achieved when the receiver coil faces the transmitter coil directly ( $\theta = 0^\circ$ ). Therefore, this orientation is used in prototype evaluations to ensure maximum energy transfer and system efficiency.

### 4.3 Effect of Air-Gap Distance on Power Transfer

One of the key physical factors influencing the performance of a resonant inductive wireless power transfer system is the distance between the transmitter and receiver coils. Theoretically, the strength of magnetic coupling between the coils and consequently the voltage induced at the receiver decreases as the separation between coils increases. This experiment was conducted to validate this hypothesis. To examine this effect, the system was tested at different air-gap distances, from  $d_1=10\text{mm}$  all the way to  $d_7=70\text{mm}$  in intervals of 10mm. Throughout the experiment, the supply voltage and coil parameters are held constant. The output voltage across the receiver is measured at each distance using a digital multimeter. The results of the experiment are presented below.

Supply Voltage (V)	Distance between coils (mm)	Receiver Output Voltage (V)
12	10	4.37
12	20	3.64
12	30	3.07
12	40	2.60
12	50	2.48
12	60	2.35
12	70	2.22

Table 4. 2 Effect of Coil Separation on Received Output Voltage

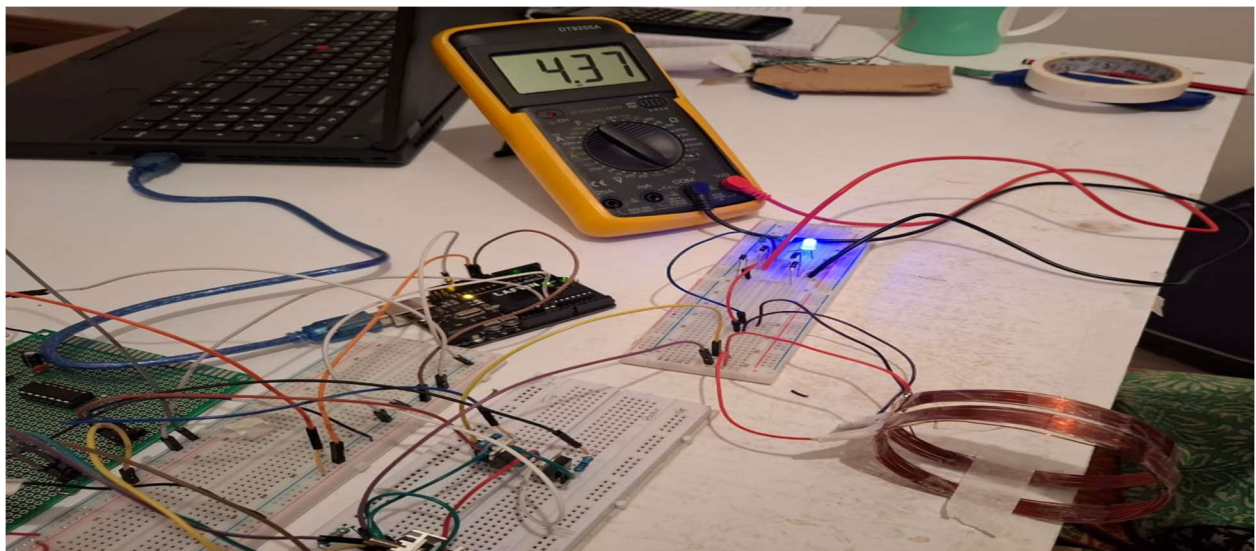


Figure 4. 3 Experimental Setup for  $d=10\text{mm}$

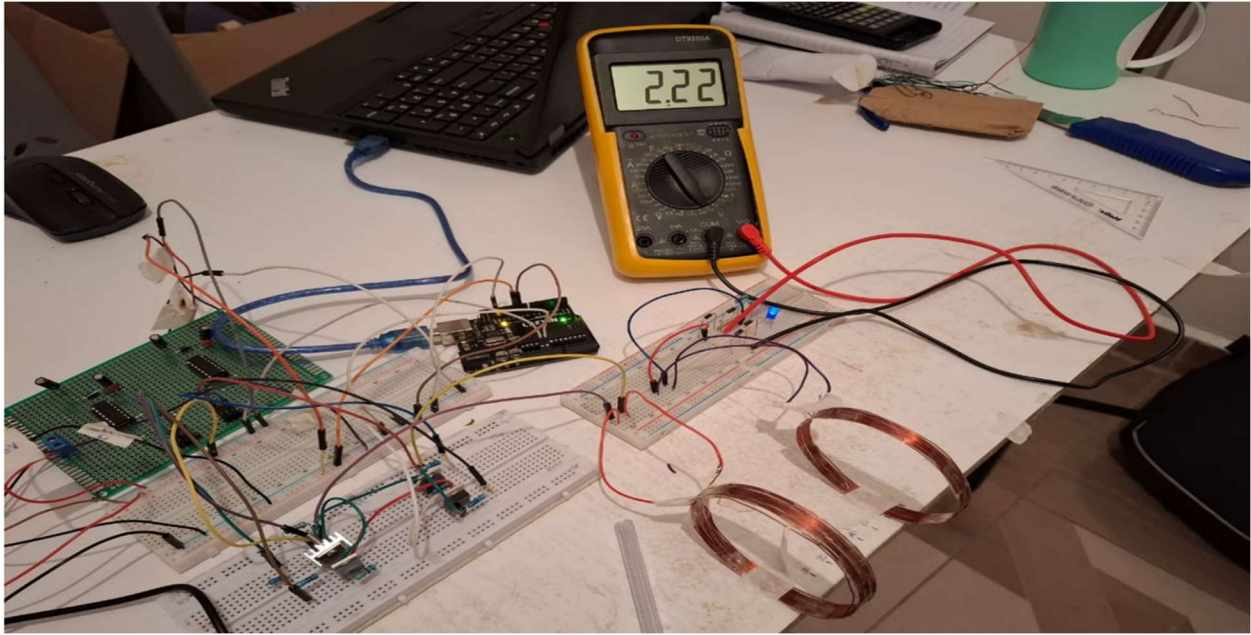


Figure 4. 4 Experimental Setup for  $d=70\text{mm}$

The results clearly demonstrate that as the distance between the coils increases, the voltage induced at the receiver decreases. When the coils are closely spaced at 10 mm, the output voltage is at its peak, indicating strong magnetic coupling. As the distance increased to 20 mm all the way to 70mm, the output voltage drops with each subsequent increase in separation distance, confirming a steady decline in coupling efficiency.

This behavior aligns with theoretical expectations based on the mutual inductance model, where coupling coefficient  $k$  diminishes as separation increases. The decrease in induced voltage is primarily due to the spread and weakening of magnetic flux with distance, reducing the amount of flux linking the receiver coil.

#### 4.4 Prototype Development

The outcomes of the preceding experiments have been critical in shaping the final prototype configuration of the wireless power transfer system. Based on the results analyzed above, the optimized electrical and geometric parameters for the prototype have been selected to maximize voltage transfer, ensure reliable performance, and maintain physical practicality.

##### 4.4.1 Transmitter Prototype Design

For the transmitter side of the prototype, the system has been designed to operate at a supply voltage of 12 V DC. This choice is based on previous experiments, where a 12 V input proved

effective in maintaining a receiver-side DC output of around 5 V, which reliably powers low-power loads such as LEDs.

The transmitter coil is constructed using 0.75 mm enameled copper wire. The 0.75 mm wire was selected due to its practicality in winding, compatibility with standard prototyping boards, and its ability to still deliver sufficient output voltage, especially when coil alignment and air gap are optimized. Since both the transmitter and receiver must resonate at the same frequency for efficient power transfer, maintaining symmetry in coil parameters is critical. Therefore, the same wire gauge, number of turns, and radius have been used on both ends.

#### 4.4.2 Receiver Prototype Design

The receiver prototype is developed to mirror the resonance and coil parameters of the transmitter, ensuring maximum power transfer through efficient magnetic coupling. The receiver circuit comprises a hand-wound coil identical to the transmitter coil, a compensation capacitor connected in a parallel-resonant configuration, and a full-bridge rectifier built using four IN5819 Schottky diodes. The rectified output is smoothed using a 470  $\mu\text{F}$  capacitor to produce a stable DC voltage across the load.

The use of identical coil dimensions and compensation capacitor values ensures that both coils resonate at the same frequency, approximately 100 kHz, allowing the system to maintain strong magnetic coupling across the selected air-gap distance. This design approach offers several benefits:

- i. Symmetry in resonance characteristics, enabling maximum power transfer at tuned frequency
- ii. Simplified tuning, as the same capacitor values can be used without complex calibration
- iii. Modularity, making the receiver easily detachable or integrable with low-power electronics

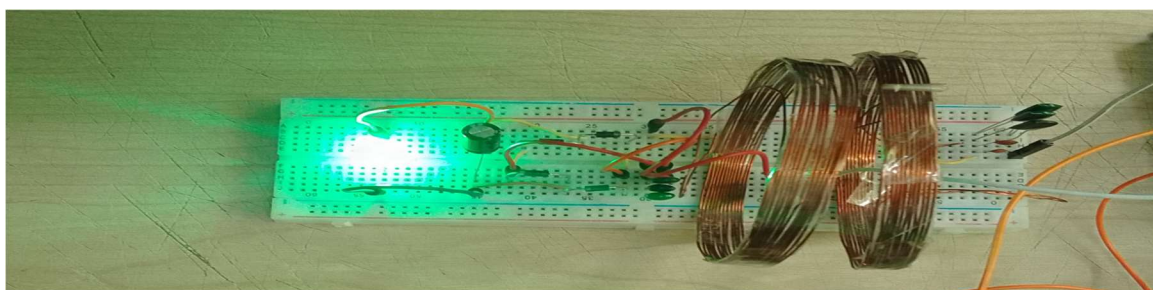


Figure 4. 5 Receiver Section

# **Chapter 5: CONCLUSION AND RECOMMENDATIONS**

## **5.1 Conclusion**

This project set out to design, implement, and experimentally evaluate a wireless power transfer system for low-power applications using resonant inductive coupling. The objective was to develop a working prototype capable of delivering usable DC power to a load without physical electrical connections. Through a systematic design process, including theoretical modeling, component selection, prototyping, and testing, the project successfully achieved its core goals.

The system was divided into a transmitter and receiver subsystem, both tuned to resonate at approximately 100 kHz. The transmitter side featured a 12 V DC input, an Arduino-controlled H-bridge inverter, and a hand-wound series-compensated LC tank coil. The receiver side consisted of a parallel-compensated coil, a full-bridge Schottky rectifier, and a smoothing capacitor supplying power to an LED and other low-power loads.

Experimental testing demonstrated that:

- i. The system could reliably transfer power across an air gap of up to 70 mm, with best performance achieved below 40 mm.
- ii. Receiver output voltages of ~5V were consistently achieved under typical alignment and load conditions.
- iii. Magnetic coupling was highly sensitive to coil alignment and orientation, confirming theoretical expectations.

Key components such as the IR2110 gate drivers, IRFZ44N MOSFETs, and NP0 capacitors proved effective in real-world operation. The use of hand-wound coils, supported by online inductance estimation, was sufficient for tuning and achieving resonance. Despite minor limitations in efficiency and load variability, the system demonstrated strong proof-of-concept performance, validating resonant inductive coupling as a viable method for low-power wireless energy transfer.

## **5.2 Recommendations**

Although the system performed successfully as a prototype, several opportunities for enhancement and further exploration remain:

### i. Closed Loop Control and Load Detection

In its current form, the system operates in open-loop, continuously transmitting power regardless of load presence. Incorporating load detection sensors such as current sensing via ACS712 could allow the system to activate transmission only when a receiver is present, improving energy efficiency and reducing thermal buildup.

### ii. Automatic Frequency Tracking

Minor deviations in coil properties or alignment can shift the resonant frequency. Future iterations could implement automatic frequency sweeping and locking using microcontroller-based feedback for example peak voltage detection or impedance phase monitoring to dynamically tune the PWM frequency for optimal resonance.

### iii. Thermal and Overvoltage Protection

Although thermal performance was within safe limits, integrating overtemperature shutdown and receiver-side voltage regulation via LDOs or TVS diodes would improve long-term reliability and protect sensitive loads.

### iv. Printed Coils or Commercial Qi Coils

To minimize variability in inductance and improve compactness, future designs could utilize commercial Qi-compatible coils or planar PCB spiral coils with known inductance values. This would enhance reproducibility and potentially improve efficiency through reduced AC resistance.

### v. Wireless Communication Integration

Integrating Bluetooth Low Energy (BLE) or LoRa modules into the microcontroller could enable remote monitoring or feedback control of power flow, especially in IoT or mobile charging applications

### vi. Efficiency Optimization

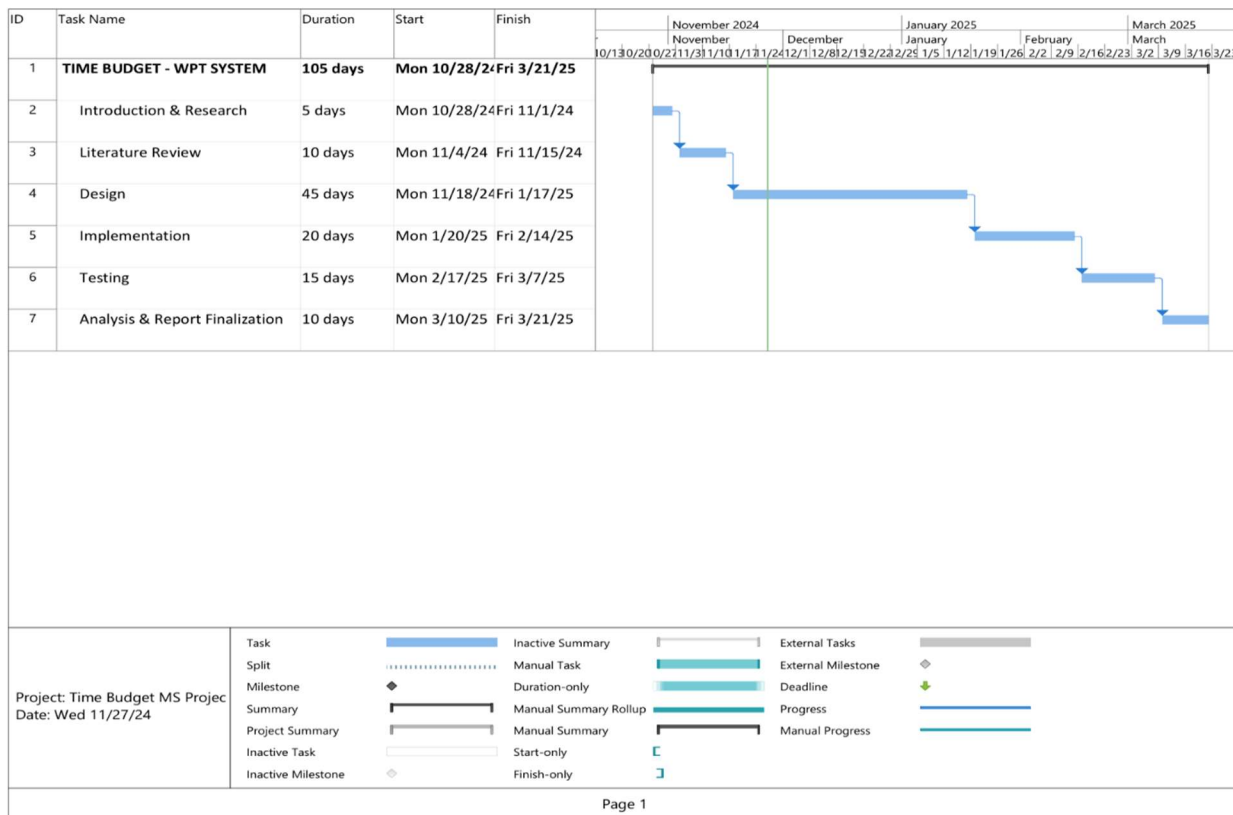
Advanced simulations and experimentation with different compensation topologies such as the LCL network as well as better coil geometries and alignment aids, could yield higher power transfer efficiency for practical deployment.

### 5.3 Final Remarks

This project demonstrated the feasibility, flexibility, and educational value of resonant inductive wireless power transfer for low-power applications. The prototype serves as a foundational platform upon which more advanced systems—incorporating intelligence, adaptivity, and higher efficiency—can be built. With further refinement and integration, such systems have significant potential in IoT, wearable devices, medical sensors, and wireless charging platforms, helping eliminate cable dependence and improve user experience in the era of smart electronics.

## APPENDICES

### TIME BUDGET



### PHOTOGRAPHIC DOCUMENTATION OF COIL ORIENTATION EXPERIMENTS

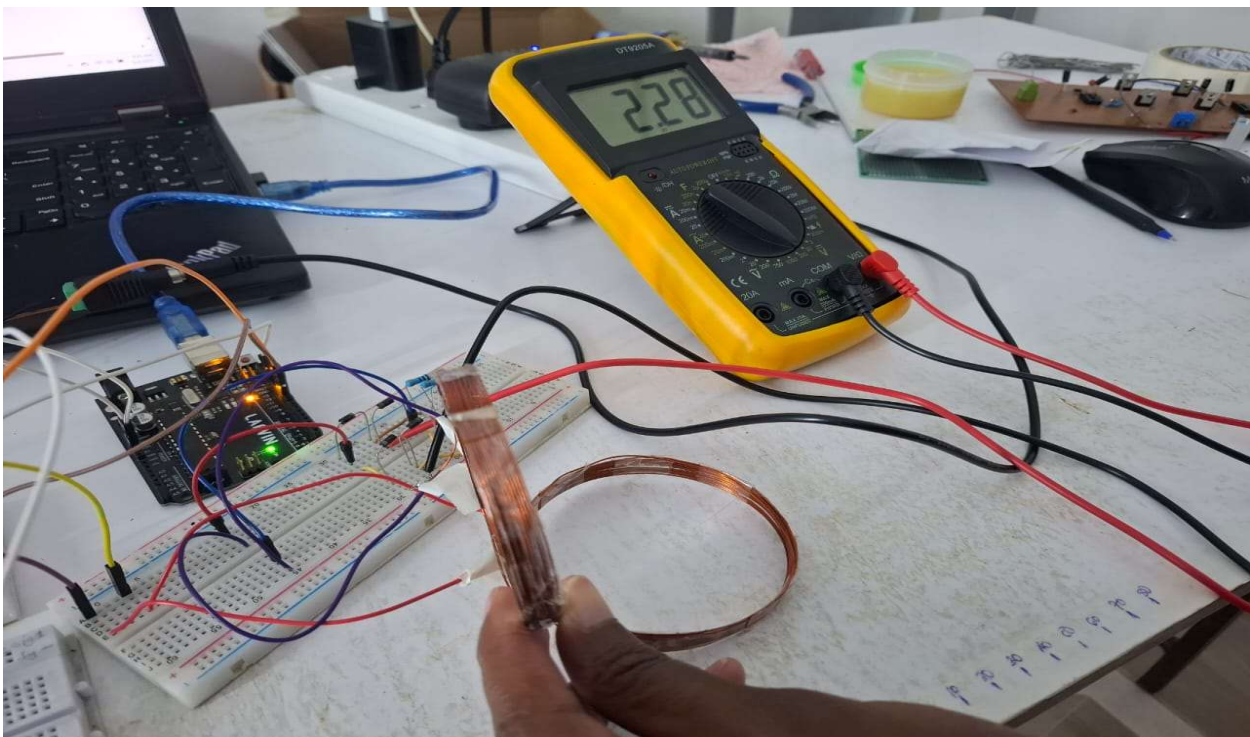
#### Coils Aligned at 0°



**Coils Aligned at 45°**

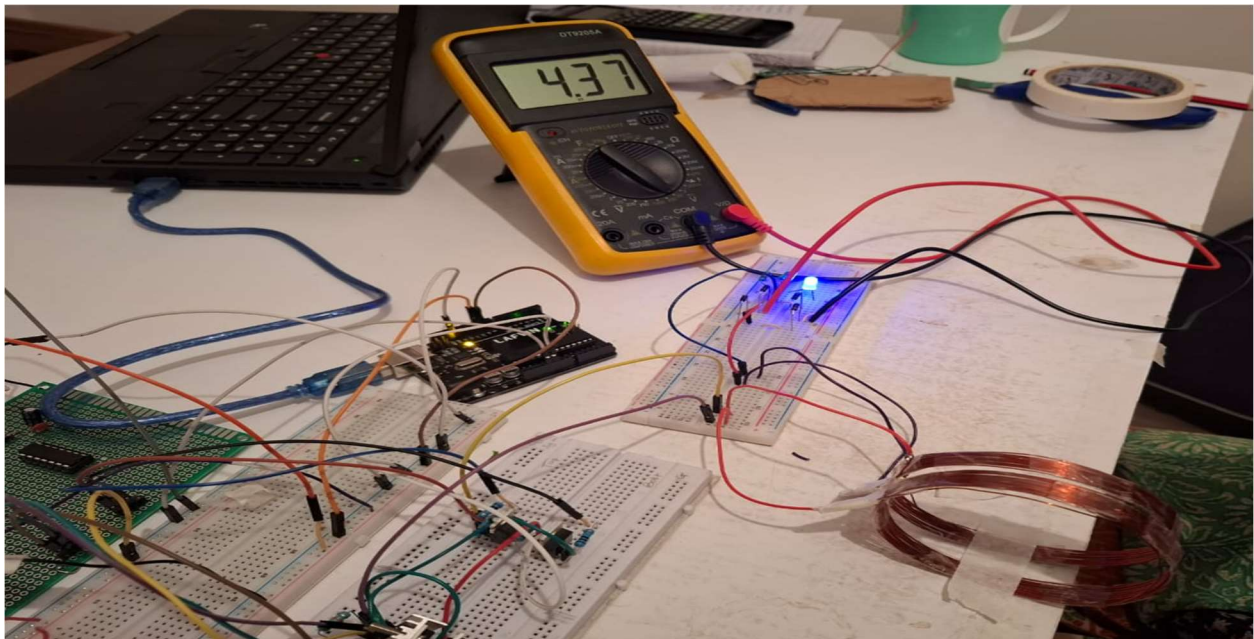


**Coils Aligned at 90°**

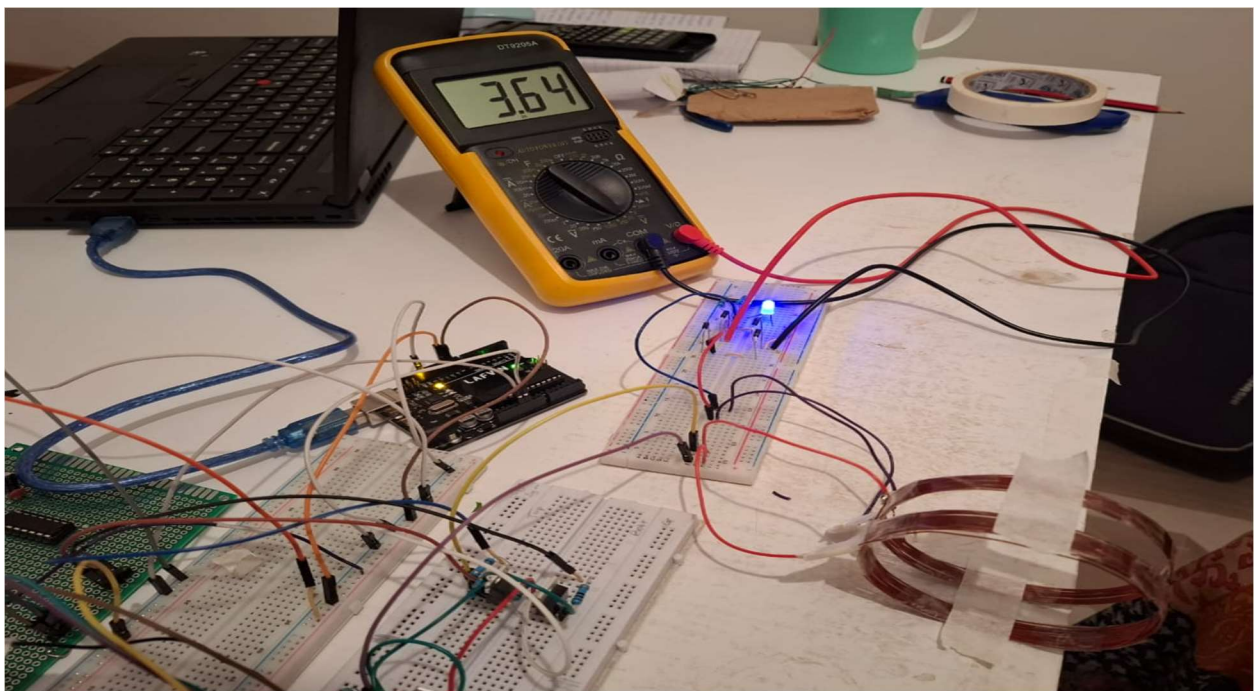


## COIL SEPARATION DISTANCE TEST IMAGES

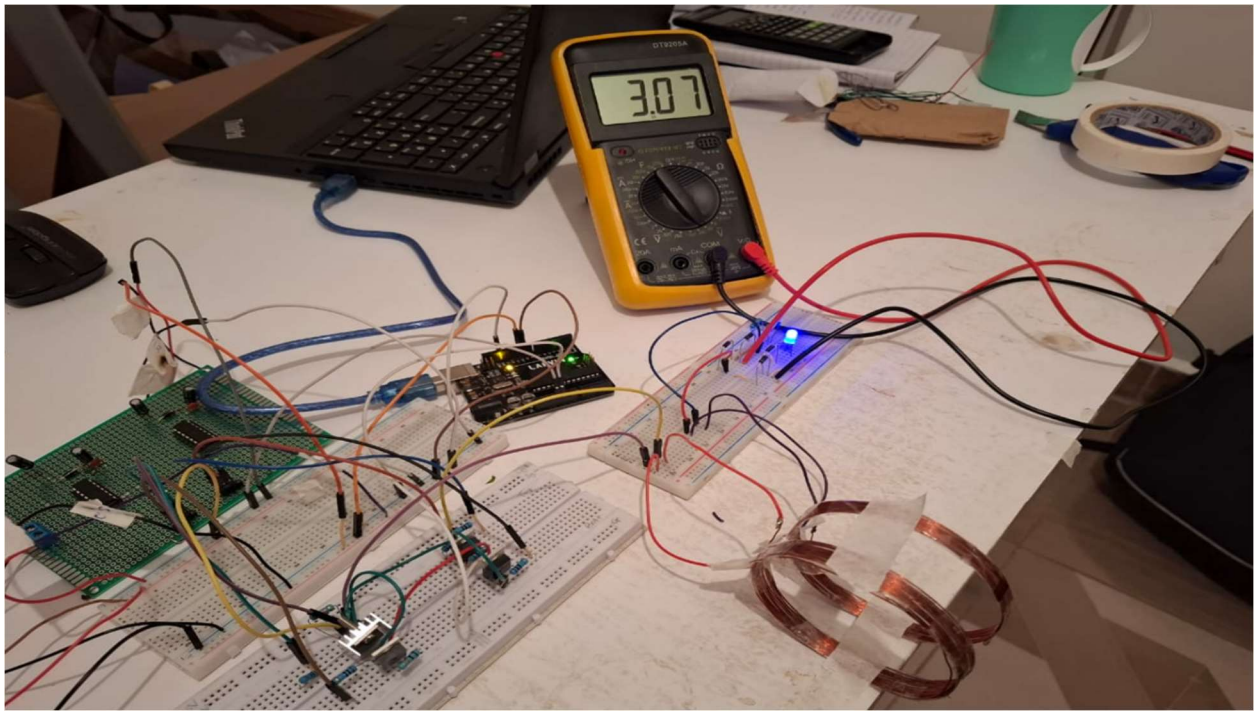
Separation Distance = 10mm



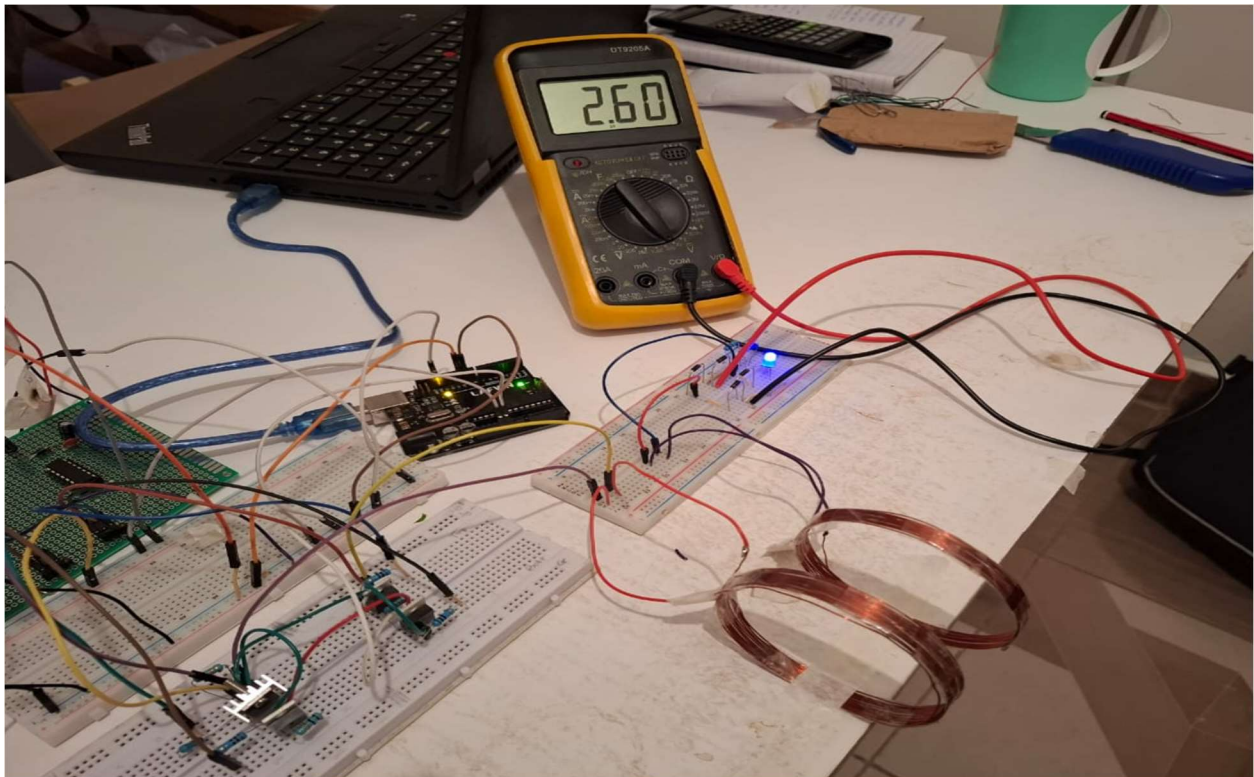
Separation Distance = 20mm



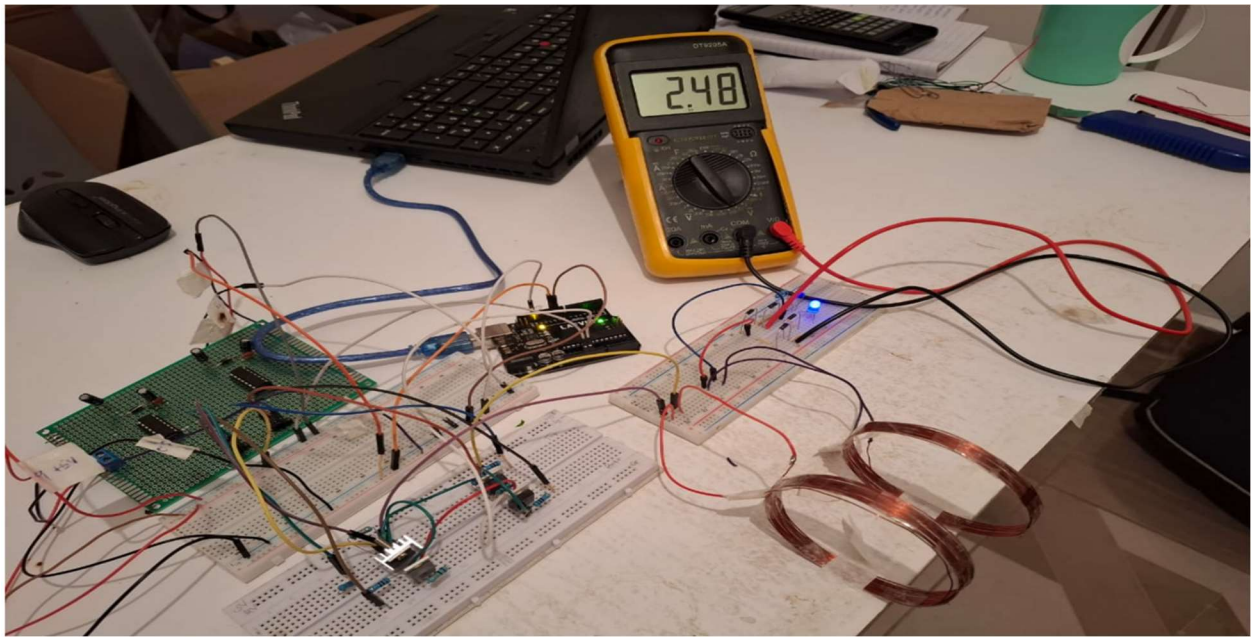
**Separation Distance = 30mm**



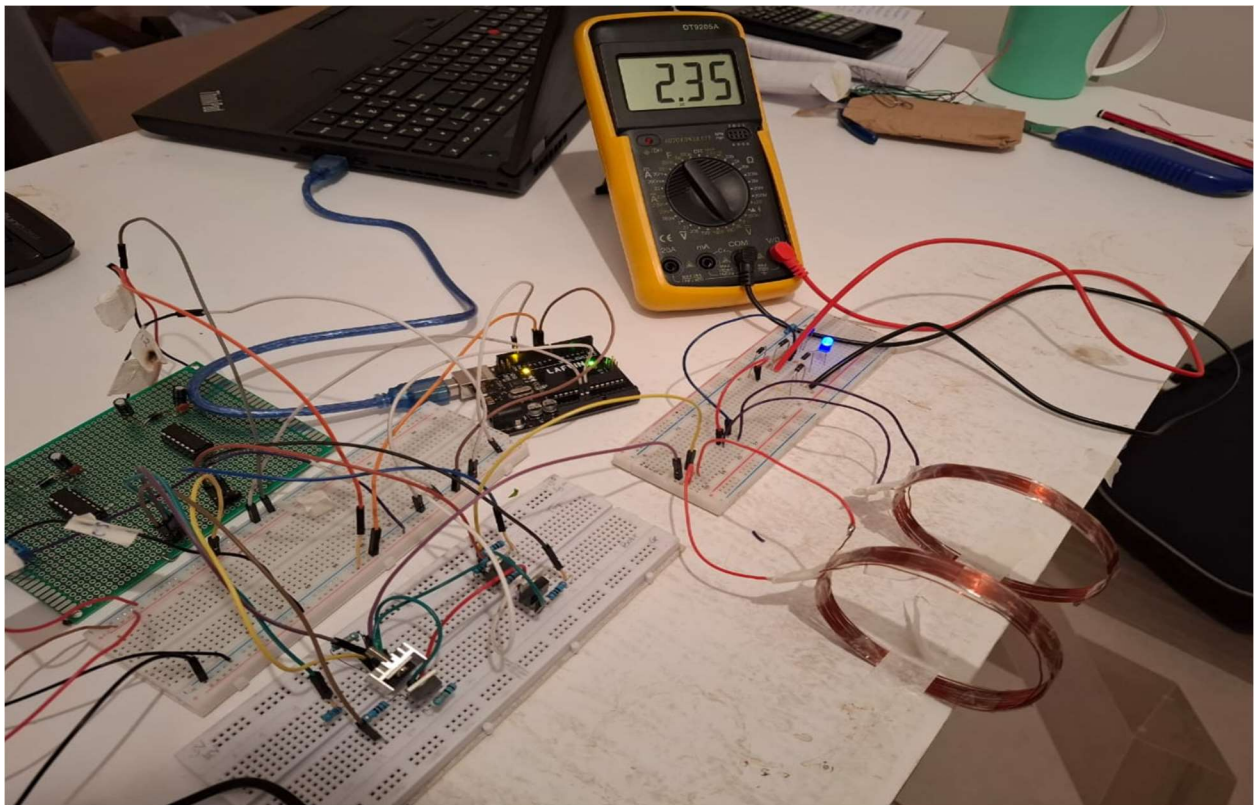
**Separation Distance = 40mm**



**Separation Distance = 50mm**



**Separation Distance = 60mm**



## REFERENCES

- [1] N. Shinohara, Ed., *Wireless power transfer: theory, technology, and applications.* in IET energy engineering series, no. 112. London: Institution of Engineering and Technology, 2018.
- [2] K. Detka and K. Górecki, “Wireless Power Transfer—A Review,” *Energies*, vol. 15, no. 19, Art. no. 19, Jan. 2022, doi: 10.3390/en15197236.
- [3] E. Coca, Ed., *Wireless Power Transfer - Fundamentals and Technologies*. InTech, 2016. doi: 10.5772/61488.
- [4] I. Adam, K. A. Kadir, S. Khan, A. Nurashikin, and H. Mansor, “Inductive resonant power transfer and topology consideration,” in *2017 IEEE 3rd International Conference on Engineering Technologies and Social Sciences (ICETSS)*, Bangkok: IEEE, Aug. 2017, pp. 1–5. doi: 10.1109/ICETSS.2017.8324197.
- [5] M. Heidarian, S. J. Burgess, R. Prabhu, and N. Fough, “Optimal Coil Design for Maximum Power Transfer Efficiency in Resonantly Coupled Systems,” in *2019 USNC-URSI Radio Science Meeting (Joint with AP-S Symposium)*, Jul. 2019, pp. 73–74. doi: 10.1109/USNC-URSI.2019.8861834.
- [6] Y. Ben Fadhel, S. Ktata, S. Rahmani, and K. Al-Haddad, “Design of a wireless power transmission system using ZVS technique and the resonant inductive coupling with hiltting the influence of the distance on the transfer efficiency,” in *IECON 2017 - 43rd Annual Conference of the IEEE Industrial Electronics Society*, Beijing: IEEE, Oct. 2017, pp. 5336–5341. doi: 10.1109/IECON.2017.8216924.
- [7] S. Gaurav, C. Kumar, and A. Meena, “LCL-LCL Topology based Resonant Inductive Wireless Power Transfer System,” in *2023 11th National Power Electronics Conference (NPEC)*, Guwahati, India: IEEE, Dec. 2023, pp. 1–6. doi: 10.1109/NPEC57805.2023.10385024.
- [8] M. A. Budak, H. Mese, and E. Durna, “A Complete Design of Series Resonant Inductive Wireless Power Transfer System for Battery-Less Systems,” in *2022 9th International Conference on Electrical and Electronics Engineering (ICEEE)*, Alanya, Turkey: IEEE, Mar. 2022, pp. 250–254. doi: 10.1109/ICEEE55327.2022.9772543.
- [9] S. Gaurav, C. Kumar, and A. Meena, “Coil Coupling Design for Resonant Inductive Wireless Power Transfer System,” in *2023 11th National Power Electronics Conference (NPEC)*, Guwahati, India: IEEE, Dec. 2023, pp. 1–6. doi: 10.1109/NPEC57805.2023.10384907.
- [10] S. Ansari, A. Das, and A. Bhattacharya, “Resonant Inductive Wireless Power Transfer of Two-Coil System with Class-E Resonant High Frequency Inverter,” in *2019 6th International Conference on Signal Processing and Integrated Networks (SPIN)*, Noida, India: IEEE, Mar. 2019, pp. 269–273. doi: 10.1109/SPIN.2019.8711782.
- [11] Y. Li, J. Hu, X. Li, H. Wang, and K. W. E. Cheng, “Cost-Effective and Compact Multistring LED Driver Based on a Three-Coil Wireless Power Transfer System,” *IEEE Trans. Power Electron.*, vol. 34, no. 8, pp. 7156–7160, Aug. 2019, doi: 10.1109/TPEL.2019.2899454.
- [12] S. Chatterjee, A. Iyer, C. Bharatiraja, I. Vagharia, and V. Rajesh, “Design Optimisation for an Efficient Wireless Power Transfer System for Electric Vehicles,” *Energy Procedia*, vol. 117, pp. 1015–1023, Jun. 2017, doi: 10.1016/j.egypro.2017.05.223.
- [13] H. Pandey, K. K. Singh, S. Sakalkar, G. Yadav, and M. Singh, “Enhancing Wireless Charging for Electric Vehicles: A Comparative Study of Coil Designs and Their Impact on Power Transfer Efficiency,” in *2024 IEEE Third International Conference on Power*

- Electronics, Intelligent Control and Energy Systems (ICPEICES)*, Delhi, India: IEEE, Apr. 2024, pp. 1207–1212. doi: 10.1109/ICPEICES62430.2024.10719184.
- [14] P. Jayathurathnage, A. Alphones, and H. Shimasaki, “Coil design guidelines for high efficiency of wireless power transfer (WPT),” Nov. 2016, pp. 726–729. doi: 10.1109/TENCON.2016.7848098.
  - [15] T. Honjo, T. Koyama, K. Umetani, and E. Hiraki, “Novel receiving coil structure for improving efficiency and power transfer capability of resonant inductive coupling wireless power transfer”.
  - [16] A. K. Loganathan and K. Subramanian, “Design of Inductive Resonance Coupling-based Wireless Charging Infrastructure for Electric Vehicles,” in *2022 International Conference and Utility Exhibition on Energy, Environment and Climate Change (ICUE)*, Pattaya, Thailand: IEEE, Oct. 2022, pp. 1–8. doi: 10.1109/ICUE55325.2022.10113502.
  - [17] C. Nataraj, S. Khan, M. H. Habaebi, A. G. A. Muthalif, and A. Arshad, “Resonant coils analysis for inductively coupled wireless power transfer applications,” in *2016 IEEE International Instrumentation and Measurement Technology Conference Proceedings*, Taipei, Taiwan: IEEE, May 2016, pp. 1–6. doi: 10.1109/I2MTC.2016.7520343.
  - [18] J. M. Romero-Arguello, A.-V. Pham, C. S. Gardner, and B. Funsten, “Miniature Coil Design for Through Metal Wireless Power Transfer,” in *2021 IEEE Wireless Power Transfer Conference (WPTC)*, San Diego, CA, USA: IEEE, Jun. 2021, pp. 1–4. doi: 10.1109/WPTC51349.2021.9458148.